

Exploring derivatives of quinazoline alkaloid l-vasicine as cap groups in the design and biological mechanistic evaluation of novel antitumor histone deacetylase inhibitors

Mudassier Ahmad, Mushtaq A. Aga, Javeed Ahmad Bhat, Brijesh Kumar, Abdul Rouf, Neena Capalash, Mubashir Javeed Minto, Ashok Kumar, Priya Mahajan, Dilip Manikrao Mondhe, Amit Nargotra, Parduman Raj Sharma, Mohmmad Afzal Zargar, Ram A. Vishwakarma, Bahawal Ali Shah, Subhash Chandra Taneja, and Abid Hamid

J. Med. Chem., **Just Accepted Manuscript** • DOI: 10.1021/acs.jmedchem.7b00322 • Publication Date (Web): 03 Apr 2017

Downloaded from <http://pubs.acs.org> on April 4, 2017

Just Accepted

“Just Accepted” manuscripts have been peer-reviewed and accepted for publication. They are posted online prior to technical editing, formatting for publication and author proofing. The American Chemical Society provides “Just Accepted” as a free service to the research community to expedite the dissemination of scientific material as soon as possible after acceptance. “Just Accepted” manuscripts appear in full in PDF format accompanied by an HTML abstract. “Just Accepted” manuscripts have been fully peer reviewed, but should not be considered the official version of record. They are accessible to all readers and citable by the Digital Object Identifier (DOI®). “Just Accepted” is an optional service offered to authors. Therefore, the “Just Accepted” Web site may not include all articles that will be published in the journal. After a manuscript is technically edited and formatted, it will be removed from the “Just Accepted” Web site and published as an ASAP article. Note that technical editing may introduce minor changes to the manuscript text and/or graphics which could affect content, and all legal disclaimers and ethical guidelines that apply to the journal pertain. ACS cannot be held responsible for errors or consequences arising from the use of information contained in these “Just Accepted” manuscripts.

SCHOLARONE™
Manuscripts

1
2
3
4
5
6
7
8
9
10
11
12
13
14
15
16
17
18
19
20
21
22
23
24
25
26
27
28
29
30
31
32
33
34
35
36
37
38
39
40
41
42
43
44
45
46
47
48
49
50
51
52
53
54
55
56
57
58
59
60

1
2
3
4 Exploring derivatives of quinazoline alkaloid *l*-
5
6
7
8 vasicine as cap groups in the design and biological
9
10
11
12 mechanistic evaluation of novel antitumor histone
13
14
15
16
17 deacetylase inhibitors
18
19
20

21
22 Mudassier Ahmad,^{1,†} Mushtaq A. Aga,^{1,†} Javeed Ahmad Bhat,^{1,‡,§} Brijesh Kumar,[†] Abdul Rouf[†]
23
24 Neena Capalash,[‡] Mubashir Javeed Minto,^{‡,§} Ashok Kumar,[†] Priya Mahajan,[¥] Dilip Manikrao
25
26 Mondhe,^{‡,§} Amit Nargotra,[¥] Parduman Raj Sharma,^{‡,§} Mohmmad Afzal Zargar,[‡] Ram A.
27
28 Vishwakarma,[#] Bhahwal Ali Shah,^{*†,§} Subhash Chandra Taneja,^{*†} Abid Hamid^{*‡,§}
29
30
31
32
33
34

35
36 [‡]Cancer Pharmacology Division, CSIR-Indian Institute of Integrative Medicine, Canal Road,
37
38 Jammu-180001, India.

39
40 [†]Natural Product Microbes Division,[#] Medicinal Chemistry Division, CSIR-Indian Institute of
41
42 Integrative Medicine, Canal Road, Jammu-180001, India.

43
44 [¥]Discovery Informatics Division, CSIR-Indian Institute of Integrative Medicine, Canal Road,
45
46 Jammu-180001, India.

47
48 [‡]Department of Biochemistry, University of Kashmir-190006, India

49
50 [‡]Department of Biotechnology, Panjab University, Chandigarh-160014, India

51
52 [§]CSIR-Academy of Scientific & Innovative Research, New Delhi, Govt. of India.
53
54
55
56
57
58
59
60

Abstract

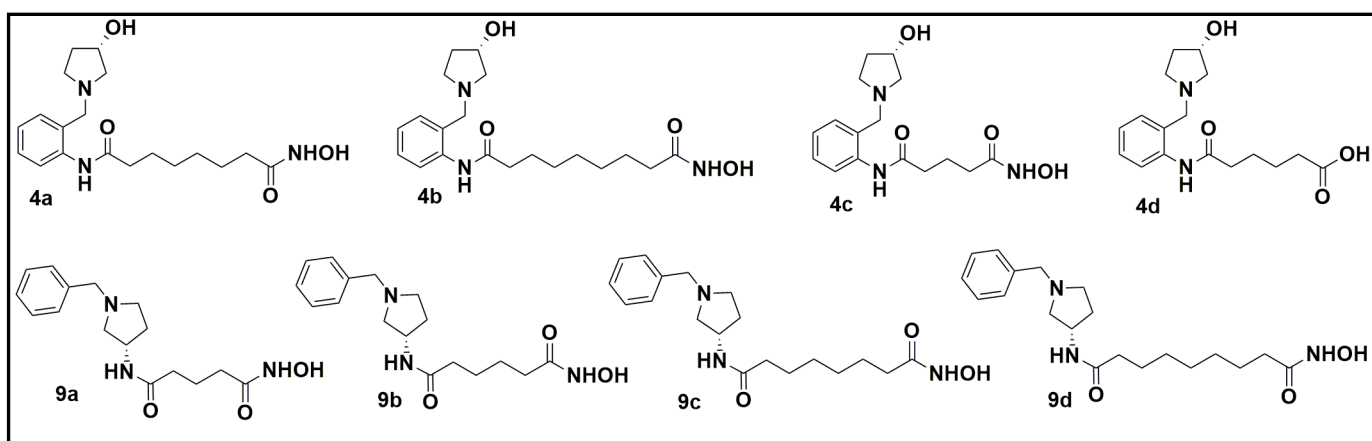
1
2
3
4
5
6
7 *l*-Vasicine is a quinazoline alkaloid with electron dense ring and additional functionalities in its
8 structure. Employing target oriented synthesis (TOS) based on in silico studies, molecules with
9 significant docking scores containing different derivatives of *l*-vasicine as caps were synthesized.
10 Interestingly, one molecule i.e., **4a** which contained 3-hydroxypyrrolidine as a cap group and six
11 carbon long aliphatic chain as a linker was found to inhibit HDACs. **4a** showed more specificity
12 towards class I HDAC isoforms. Also **4a** was found to be less cytotoxic towards normal cell
13 lines as compared to cancer cell lines. **4a** inhibited cancer cell growth and induced cell death by
14 various mechanisms. However, **4a** was found to induce cell death independent of ROS
15 generation and unlike many natural product based HDAC inhibitors; **4a** was found to be non-
16 toxic under in vivo conditions. Importantly, we for the first time report the possibility of using 3-
17 hydroxypyrrolidine a cap for the synthesis of HDAC inhibitors with good potency.
18
19
20
21
22
23
24
25
26
27
28
29
30
31
32
33
34
35
36
37
38
39
40
41
42
43
44
45
46
47
48
49
50
51
52
53
54
55
56
57
58
59
60

Introduction

In cancer, epigenetics has been found to play an important role in the origin, development and metastasis^{1,2}. Last decade has also witnessed clinical applications of epigenetics in cancer. Epigenetic writer and reader enzymes like histone deacetylases (HDACs), DNA methyl transferases (DNMTs), histone methyl transferases (HMTs) are being increasingly used as targets for chemotherapeutic intervention in cancer and other diseases like diabetes and neurodegenerative disorders^{3,4}. Acetylation of histones is the common epigenetic mechanism used by cells for regulating the cellular processes like gene expression, cell growth, cell death etc^{5,6}. Dysregulation of the acetylation has been associated with diverse cellular events in the cancer pathologies^{7,8}. Global hypoacetylation of H4 is the common feature of human tumours^{9,10}. Acetylation of histones and other proteins is maintained by two antagonistic families of enzymes, histone deacetylases (HDACs) and histone acetyl transferases (HATs)^{6,11}. Due to its reversible nature, acetylation has been harnessed for cancer chemotherapy^{1,12}. So far, two HDAC inhibitors suberoylanalide hydroxamic acid (SAHA) and romidepsin have already been approved by the FDA as drugs against Chronic T Cell Lymphoma (CTCL)^{13,14}. Besides, there are tens of HDAC inhibitors at various stages of clinical trials against different cancers^{11,15}. HDAC inhibitors increase the acetylation level of histones and have been chiefly found to reactivate the expression of numerous silenced genes that promotes cell death^{1,11}. HDAC inhibitors also lead to cell growth arrest, cell differentiation and angiogenesis inhibition which are important biological processes for suppression of cancers^{16,17}.

Taking into account the potential therapeutic efficacy of HDAC inhibitors, several classes of HDAC inhibitors have been designed. However in spite of large efforts the clinical potential of HDACs has not been realized yet. Natural products offer a good opportunity for the

1
2
3 design of new HDAC inhibitors. One of the important classes of bioactive natural products is
4 quinazolines. Quinazolines show potent anticancer, anti-microbial and anti-inflammatory
5 activities¹⁸. We in our current study, explored the possibility of using derivatives of quinazoline
6 alkaloid *l*-vasicine in the design of natural product based HDAC inhibitors. *l*-vasicine is a unique
7 molecule with electron dense ring system and additional functionalities in its structure, we
8 hypothesized that these structural features may be used to design new HDAC inhibitors with *l*-
9 vasicine derivatives as cap groups. Using *in silico* approach, target oriented synthesis (TOS) and
10 biological studies, *l*-vasicine derivative 3-hydroxypyrrolidine was found to act as a suitable cap
11 group in the design of a novel HDAC inhibitor (*S*)-*N*¹-hydroxy-*N*⁸-(2-((3-hydroxypyrrolidin-1-
12 yl) methyl) phenyl) octanediamide (**4a**). Figure 1 shows the chemical structures of compounds
13 **4a-4d** and **9a-9d**.
14
15
16
17
18
19
20
21
22
23
24
25
26
27
28
29



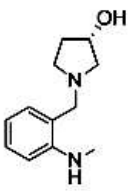
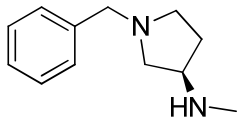
45
46
47
48
49
50
51
52
53
54
55
56
57
58
59
60

Figure 1: Chemical structures of compounds **4a-4d** and **9a-9d**

RESULTS AND DISCUSSION

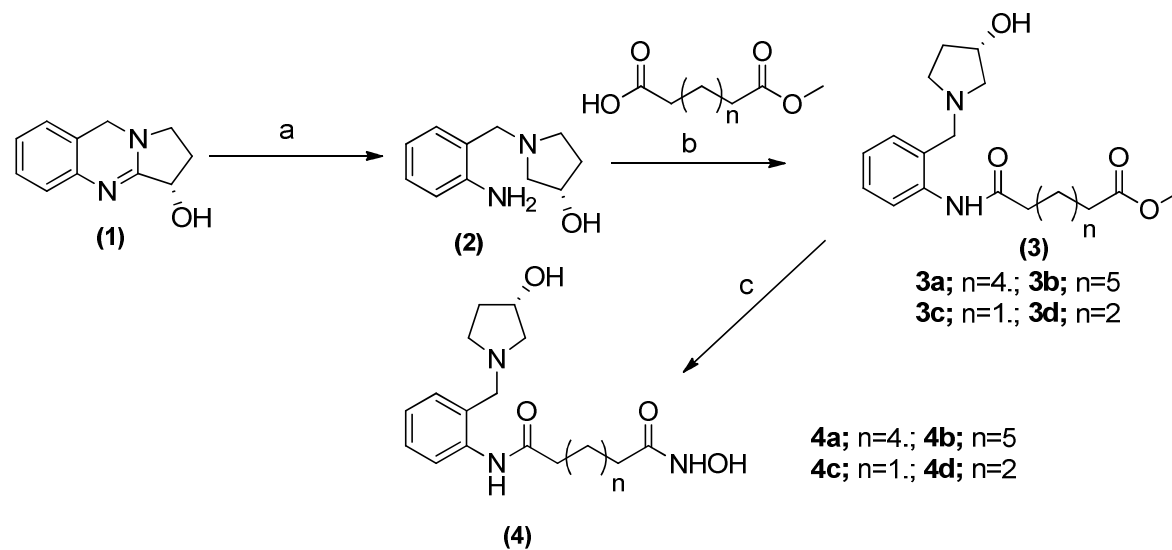
***In silico* screening of *l*-vasicine derivatives.** To support our hypothesis, different modifications of *l*-vasicine were proposed and virtual screening of proposed molecular designs was carried out. Linkers were placed on the proposed *l*-vasicine based caps at structurally and chemically feasible positions on the ring system. Hydroxamic acid was used as chelator. *In silico* studies were carried out with Schrodinger suite 2015 molecular modeling software. 3D structures of various HDAC isoforms (HDAC 1, 4 and 8) were used as receptors. Significant docking scores were achieved for *l*-vasicine derivatives (*R*)-amino-1-benzylpyrrolidine and 3-hydroxypyrrolidine when attached as cap groups to aliphatic linkers of various lengths (Table 1). The molecules which showed significant docking scores were taken as probable HDAC inhibitors and three schemes of Target Oriented Synthesis (TOS) were carried out to synthesise probable *l*-vasicine based HDAC inhibitors.

Table 1. Docking scores of novel HDAC inhibitors containing various analogs of *l*-vasicine as caps. Schrodinger suite 2015 molecular modeling software was used for *in silico* studies.

Molecule name	Cap group	Linker length	HDAC-1	HDAC-2	HDAC-4	HDAC- δ 8
4a		6 carbons	-7.5	-7.98	-6.7	-8.09
4b		7 carbons	-6.8	-7.82	-6.4	-7.69
4c		3 carbons	-7.3	-6.34	-6.0	-6.13
4d	3-hydroxy-pyrrolidine	4 carbons	-6.8	-6.89	-6.6	-7.48
9a	 (<i>R</i>)-amino-1-benzylpyrrolidine	3 carbons	-6.1	-6.88	-7.9	-6.42
9b		4 carbons	-6.6	-7.08	-7.2	-6.31
9c		6 carbons	-6.3	-7.77	-7.2	-7.82
9d		7 carbons	-6.3	-7.34	-6.7	-8.06

Chemistry

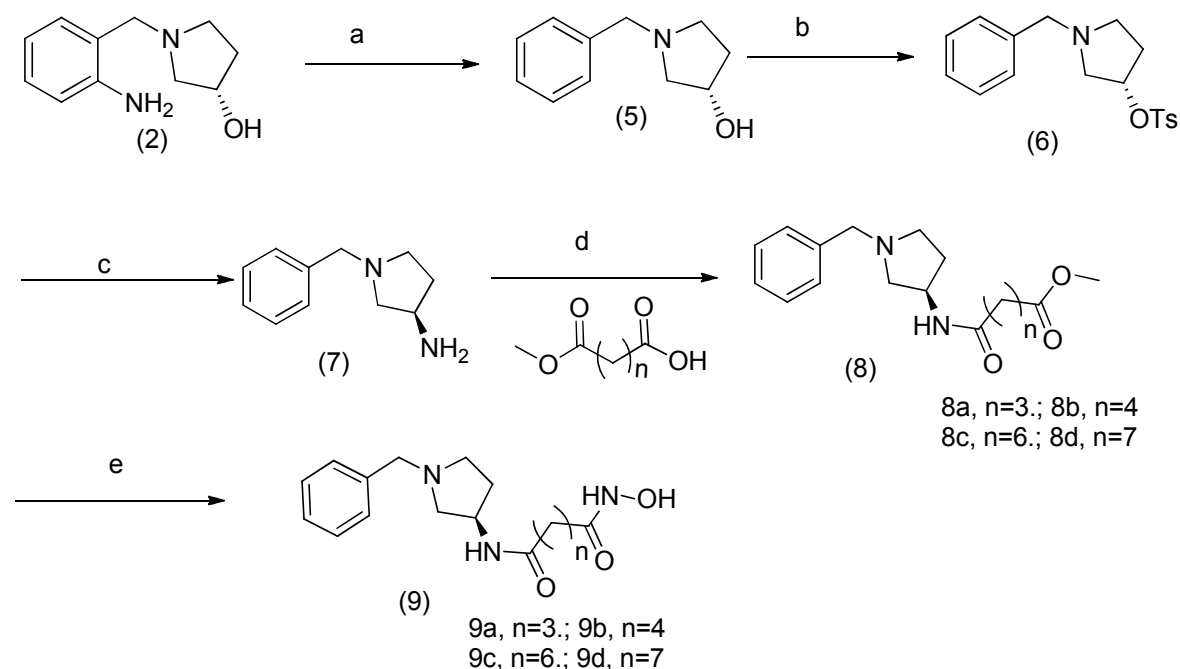
For using 3-hydroxypyrrolidine moiety as a cap region, synthesis started by bringing the cleavage of imidine bond of l-vasicine (**1**) using NaBH_4 in methanol:water (1:1) to get tetrahydrovasicine^{18, 19} (**2**). The next step was the coupling of amine (**2**) in the presence of secondary hydroxyl group with hydrophobic linker through amide bond. It would be pertinent to mention here that various hydrophobic linkers of varying chain lengths i.e., monomethyl succinic acid, monomethyl adipic acid, monomethyl suberic acid and monomethyl azealic acid were selected for these analogues. Here, boric acid mediated coupling of **2** with different linkers was found to be the best method, as it gives selectively N-coupling products i.e., **3a-3d** in the presence of a free hydroxyl group. The last step was the conversion of esters (**3a-3d**) into corresponding hydroxamic acids (**4a-d**), using hydroxylamine hydrochloride in the presence of KOH (Scheme 1).



Scheme 1. Synthesis of Histone deacetylase inhibitors from vasicine: (a) NaBH_4 , MeOH:H₂O, rt; (b) $\text{B}(\text{OH})_3$, Toluene, reflux; (c) $\text{NH}_2\text{OH}\cdot\text{HCl}$, KOH, MeOH, rt.

Besides, probable HDAC inhibitors having (*R*)-amino-1-benzylpyrrolidine (**7**) as a hydrophobic cap group were also synthesized (Scheme 2). The synthesis once again initiated

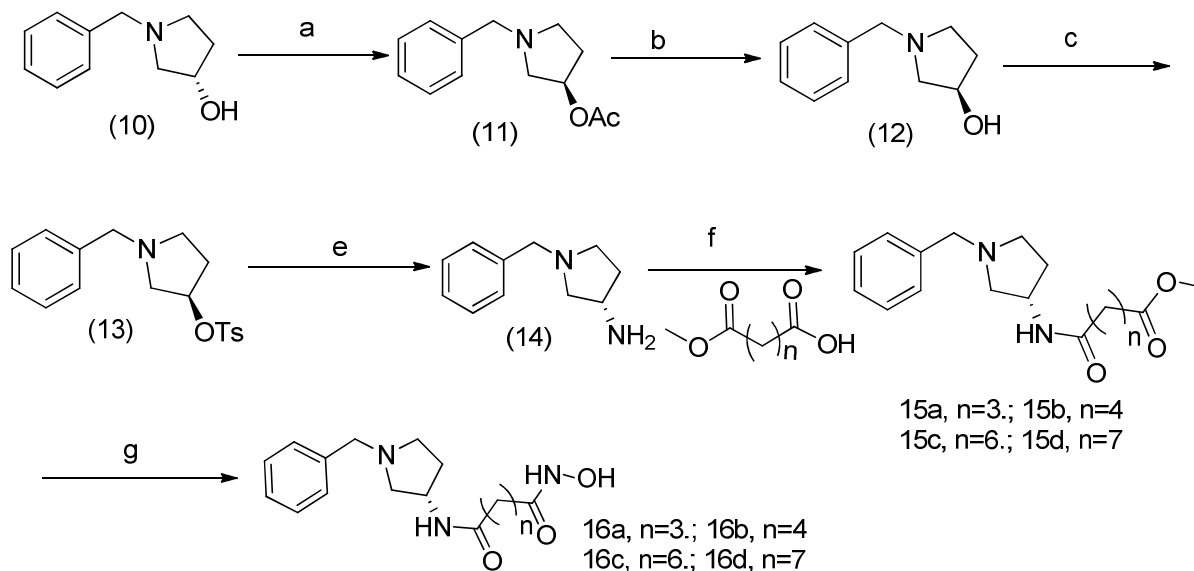
from vasicine to yield anilinic nitrogen (**2**), which on hydrodeamination (anilinic amine) in the presence of amyl nitrite gave (*S*)-1-benzylpyrrolid-3-ol (**5**). The 3-hydroxyl group of **5** was then converted into amino group (**7**) in two steps. The treatment of **5** with tosyl chloride in the presence of triethyl amine in DCM gave **6**, followed by S_N2 substitution of tosyl group in **6** with NaN₃, and thereafter *in situ* reduction of azido intermediate in the presence of PPh₃ gave (*R*)-3-amino-1-benzylpyrrolidine (**7**). Boric acid mediated coupling of **7** with the hydrophobic linker in toluene under reflux gave the esters, i.e. **8a-d**. Again, four different linkers as described in scheme 1 were attached. In the final step, the esters (**8a-d**) were converted to the corresponding hydroxamic acids (**9a-d**) by using hydroxylamine hydrochloride in the presence of KOH.



Scheme 2. Synthesis of HDAC inhibitors from (*R*)-amino-1-benzylpyrrolidine: (a) Amyl nitrite, DMF, 60 °C; (b) TsCl, TEA, DCM; (c) NaN₃, Bu₄NBr, DMF, PPh₃, 0 °C - rt; (d) B(OH)₃, Toluene, reflux; (e) NH₂OH.HCl, KOH, MeOH, rt.

Furthermore, the probable HDAC inhibitors were also synthesized *via* stereo inversion of (*S*)-1-benzylpyrrolidin-3-ol (**5**) to obtain (*R*)-1-benzylpyrrolidin-3-ol (**12**) by Mitsunobu reaction in presence of DIED, PPh₃ and acetic acid in THF. The 3-hydroxyl group of **12** was converted into

3-amine (**14**), following the two step reaction sequence depicted in **scheme 3**. Boric acid coupling of **14** with the hydrophobic linkers in toluene gave the esters **15a-d**. The esters, i.e. (**15a-d**) were converted to corresponding hydroxamic acids (**16a-d**) using hydroxylamine hydrochloride in the presence of KOH.



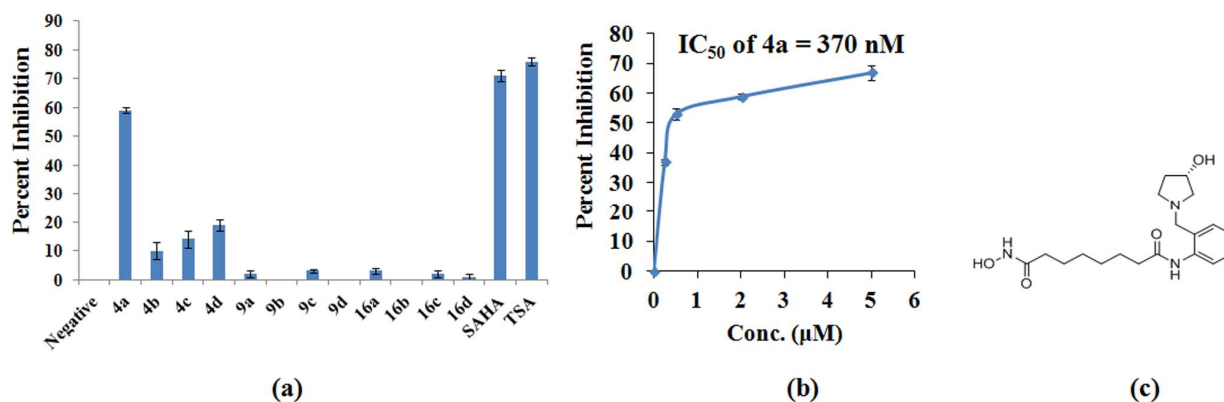
Scheme 3. Synthesis of HDAC inhibitors from (*S*)-amino-1-benzylpyrrolidine: (a) DIAD, PPh₃, AcOH, THF, 0 °C; (b) LiOH, THF, H₂O; (c) TsCl, TEA, DCM; (d) NaN₃, Bu₄NBr, DMF, PPh₃, 0 °C - rt; (e) B(OH)₃, Toluene, reflux; (f) NH₂OH.HCl, KOH, MeOH, rt.

Biological evaluation.

Screening of molecules for HDAC inhibition

The molecules with significant docking scores synthesised through above schemes of synthesis were evaluated for HDAC inhibition. First molecules were evaluated for HDAC inhibition against HeLa nuclear extract. TSA and SAHA were used as positive controls (supporting information Figure 2). HDAC inhibition activity of molecules was determined at different concentrations (0.5, 1.0, 1.5 and 2 μM concentrations) so as to generate their IC₅₀ values. The

1
2
3
4 molecules which did not show any significant HDAC inhibition up to 2 μM concentration were
5
6 taken as inactive. The results are shown in Figure 2. Molecules 9a, 9b, 9c, 9d, 16a, 16b, 16c and
7
8 16d did not show any significant HDAC inhibition up to 2 μM concentrations where as
9
10 molecules 4b, 4c and 4d showed little HDAC inhibition at this concentration. Importantly,
11
12 molecule **4a** showed significant HDAC inhibition. Molecule **4a** showed IC_{50} value of 370 nM
13
14 against the HeLa nuclear extract (Figure 2b). **4a** contains *l*-vasicine derivative 3-
15
16 hydroxypyrrolidine as a cap which proves our hypothesis. Furthermore, HDAC inhibition
17
18 activity of 3-hydroxypyrrolidine cap based molecules (**4a**, 4b, 4c and 4d) varied with any change
19
20 activity of 3-hydroxypyrrolidine cap based molecules (**4a**, 4b, 4c and 4d) varied with any change
21
22 in linker lengths. Linker length of six carbons (present in **4a**) was found suitable for HDAC
23
24 inhibition and any change in linker length rendered the molecule inactive. 3-hydroxypyrrolidine
25
26 cap based molecule with seven carbon (4b), three carbon (4c) and four carbon (4d) long linkers
27
28 cap based molecule with seven carbon (4b), three carbon (4c) and four carbon (4d) long linkers



were found to be inactive against HDACs.

Figure 2. (a) HDAC inhibition activities of the designed compounds at 2 μM concentration against HeLa nuclear extract. SAHA and TSA were used as positive controls at 20 μM concentrations. (b) HDAC inhibition curve of active molecule **4a**. **4a** showed IC_{50} value of 370 nM against HeLa nuclear extract. (c) Structure of active molecule **4a**.

Evaluation of HDAC isoform specificity of 4a

After initial screening against HeLa nuclear extract, HDAC inhibition activity of active molecule **4a** was evaluated against HDAC isoforms. SAHA was used as a positive control. The results are shown in Table 2 below. **4a** exhibited interesting HDAC isoform specificity. **4a** was found most active against HDAC isoforms 1, 2, 3 and 8 with IC₅₀ values 415, 268, 368 and 211 nM respectively. **4a** was found to be moderately active against HDAC isoforms 4 and 5 with IC₅₀ values in micro molar range while as **4a** was found to be least potent against HDAC 9, 10 and 11. These results indicate that **4a** is more active towards class I HDACs as compared to other HDACs.

Table 2. HDAC inhibition activities (IC₅₀) of 4a and SAHA against HDAC isoforms. Values are mean of three experiments and the standard error of the IC₅₀ was generally less than 10%.

Molecule	IC ₅₀ (nM)									
	Class I				Class IIa			Class IIb	Class IV	
	HDAC 1	HDAC 2	HDAC 3	HDAC 8	HDAC 4	HDAC 5	HDAC 9	HDAC 10	HDAC 11	
4a	415	268	368	211	7120	5391	>10000	>10000	>10000	
SAHA	150	454	261	300	>10000	2180	>10000	982	>10000	

Molecular modeling studies of 4a

Incorporation of linker chain and hydroxamic acid functionality to cap group (i.e. *l*-vasicine and its derivative 3-hydroxypyrrolidine) led to the identification of series of compounds with varying affinity for the HDAC-8 enzyme. The optimized novel HDAC inhibitor (*S*)-*N*¹-hydroxy-*N*⁸-(2-((3-hydroxypyrrolidin-1-yl) methyl) phenyl) octane diamide (**4a**), displayed *in-vitro* IC₅₀ value of 211 nM for HDAC-8 and 268 nM for HDAC-2. The results of molecular docking studies of **4a** are in close agreement with the *in-vitro* studies where **4a** display selectivity for HDAC-8 inhibition, in contrast to other HDACs.

1
2
3 Upon docking studies, it was observed that entire **4a** molecule was involved in interaction with
4 the HDAC-8, 3-hydroxypyrrolidine ring acts as cap group for molecular recognition and
5 involved in H-bonding with Phe-152 backbone amide. Similar to the CRAA-A and HDAC-8
6 crystal structure, drift in Phe-152 side chain creates hydrophobic sub-pocket, which provides
7 additional stability to the ligand-receptor interactions. At biological pH pyrrolidine nitrogen,
8 atom gets protonated and forms a hydrogen bond with the Tyr-111 phenolic hydroxyl group. In
9 addition to this, protonated cation is also able to interact with the Trp-141 π clouds. Similar to
10 well-known HDAC inhibitors like SAHA and CRAA-A the 6-carbon chain length linker region
11 is quiet flexible and well accommodated in the hydrophobic tunnel. In addition to the H-bonding
12 interactions with the Tyr-306 and His-142; the terminal hydroxamic acid functionality is also
13 capable of forming co-ordination bond with the Zn^{2+} metal ion.
14
15
16
17
18
19
20
21
22
23
24
25
26
27
28
29

30 Overall, the introduction of *l*-vasicine and its derivatives as cap group in the suitably designed
31 linker and metal chelator (such as hydroxamic acid) can regulate the deacetylation of the histone-
32 DNA assembly. The observed little selectivity of **4a** towards the HDAC-8 over HDAC-2 is
33 might be due to the H-bonding and π -cationic interactions of the protonated pyrrolidine nitrogen
34 with Tyr-111 and Trp-141, respectively. These interactions were not possible in case of HDAC-
35 2 because Tyr-111 and Trp-141 residues are replaced Phe-103 and Leu-133, respectively. 2D and
36 3D interactions of the **4a** with HDAC-8 are shown in Figure 3A and 3B while 2D interactions of
37 **4a** with HDAC-2 is shown in Supporting information section Figure S2.
38
39
40
41
42
43
44
45
46
47
48
49

50 **Screening of molecules for cytotoxicity**

51 **4a** and other 3-hydroxypyrrolidine cap based molecules (4b, 4c and 4d) were evaluated for
52 cytotoxicity potential against a panel of human cancer cell lines. The cells of different tissue
53 origins were included in the panel. The panel consisted of leukemia cell lines (THP-1 and HL-
54
55
56
57
58
59
60

60), colon cancer cell lines (Colo-205 and Caco-2), pancreatic cancer cell line (MIAPaCa-2), prostate cancer cell line (PC-3), lung cancer cell line (A549) and breast cancer cell line (MCF-7). The cytotoxicity of molecules was initially determined at 10 μM concentration (Table 3). Out of molecules **4a**, **4b**, **4c** and **4d**, only **4a** showed significant cytotoxicity against all the cell lines in

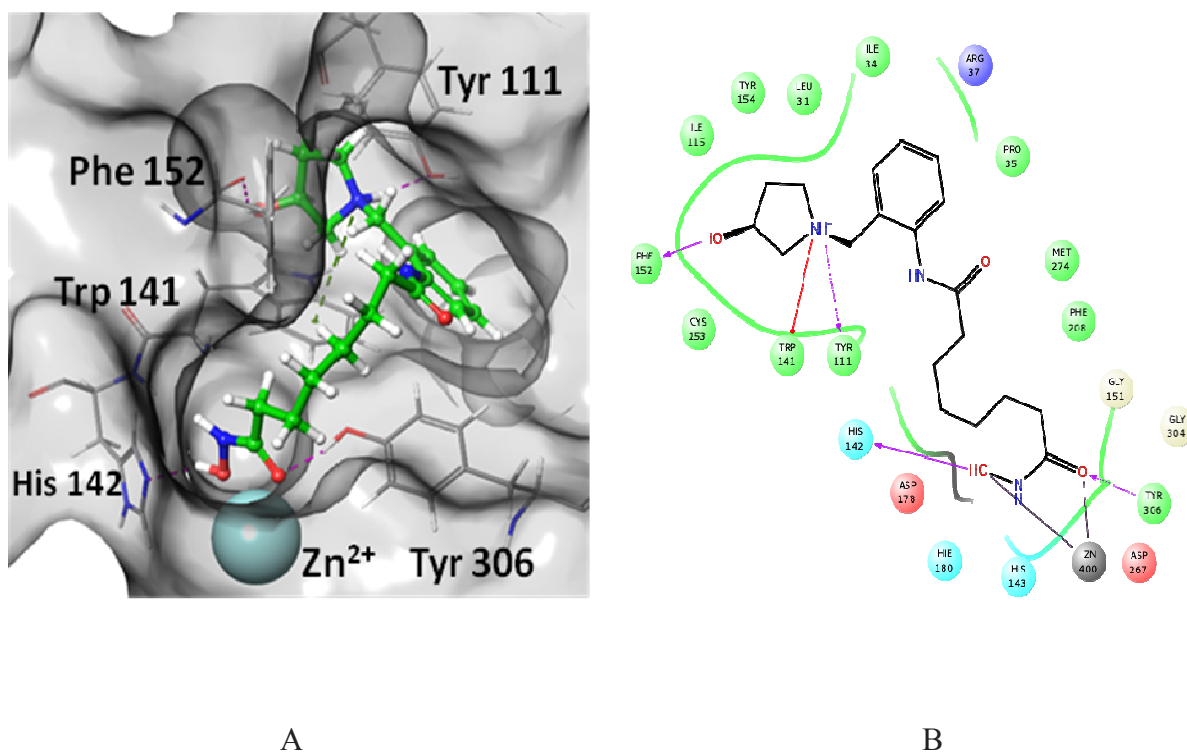


Figure 3: Interactions of 4a with HDAC-8 (PDB-1VKG), A; 3D representation, B; 2D representation.

the panel and the molecules **4b**, **4c** and **4d** were found to be inactive against all the cell lines in panel (Table 3). Importantly, **4a** is a HDAC inhibitor thus cytotoxicity of **4a** against a panel of cell lines is induced by HDAC inhibition activity of **4a** and molecules other than **4a** lack significant HDAC activity and no cell death was induced by them. Moreover, cytotoxicity of **4a** was evaluated at lower concentrations to determine IC_{50} values of **4a** against the panel of cell lines (Table 4). IC_{50} value of **4a** varied from 0.6 μM to 7.0 μM against various cancer cell lines in

the panel. Some cell lines were found to be more sensitive to cytotoxicity induced by **4a**. **4a** showed least IC₅₀ value of 0.6 μM against colon cancer cell line, i.e. Colo-205. **4a** was also found to be very significantly cytotoxic against leukaemia cell lines (THP-1, HL-60 and MOLT-4), pancreatic cancer cell line (MIAPaCa-2) and breast cancer cell line MCF-7, while as it was found to be moderately active against colon cancer cell line Caco-2 and non small cell lung cancer cell line, i.e. A549. **4a** was least cytotoxic against prostate cancer cell line PC-3. This selective cytotoxic behavior of the **4a** against some cell lines in the panel may be attributed to the epigenomic and genomic profiles of these cell lines.

Table 3. Evaluation of cytotoxicity of synthesized molecules at 10 μM concentration by MTT assay. Results are Mean ± S.D of three experiments carried out in triplicates separately.

Tissue		Leukaemia			Colon	Pancreatic	Prostate	Lung	Breast	
Cancer cell type		THP1	HL-60	MOLT-4	Colo205	Caco-2	MIAPaCa- 2	PC-3	A549	MCF-7
Test molecule	Conc. (μM)	% Growth Inhibition								
4a	10	94 ± 6	95 ± 5	91 ± 3	92 ± 7	58 ± 7	93 ± 5	29 ± 3	84 ± 9	93 ± 6
4b	10	17 ± 1	6 ± 3	30 ± 2	7 ± 4	5 ± 4	2 ± 3	12 ± 2	5 ± 6	3 ± 4
4c	10	3 ± 4	3 ± 3	27 ± 1	26 ± 4	1 ± 1	4 ± 5	2 ± 2	5 ± 6	5 ± 5
4d	10	37 ± 5	29 ± 2	38 ± 4	22 ± 4	31 ± 5	12 ± 3	15 ± 4	19 ± 3	26 ± 4
SAHA	5	91 ± 4	93 ± 2	90 ± 3	88 ± 3	93 ± 4	86 ± 3	88 ± 1	95 ± 4	89 ± 6

Table 4. IC₅₀ value of 4a against the panel of cell lines. Results are Mean ± S.D of three experiments carried out in triplicates separately.

Tissue	Leukaemia			Colon	Pancreatic	Prostate	Lung	Breast	
Cancer cell type	THP1	HL-60	MOLT-4	colo-205	Caco-2	MIAPaCa-2	PC-3	A549	MCF-7
IC ₅₀ of 4a (μM)	1.3±0.3	1.0±0.2	0.81±0.3	0.6±0.1	6.0±0.8	1.0±0.2	19.0±3	7.0±1	1.5±0.1
IC ₅₀ of SAHA (μM)	1.1 ±0.2	1.0 ± 0.2	0.7 ±0.3	1.8 ±0.1	3 ± 0.6	2.2 ±0.1	3 ±0.8	1.5±0.2	0.9±0.3

Molecule 4a induced acetylation of histones

HDAC inhibitors are known to increase the acetylation level of histones^{20, 21}. In order to further confirm that molecule **4a** caused HDAC inhibition, HL-60 and MOLT-4 cells were treated with various concentrations of **4a**. Histones were extracted from treated cells and level of acetylation on H3 at lysine 18 and H4 at lysine 5 was probed. **4a** was found to increase the acetylation at both H3K18 and H4K5 residues in both the cells (Figure 4). The level of acetylation increased with increase in concentration of **4a** which further proves that **4a** is a HDAC inhibitor. SAHA was used as a positive control.

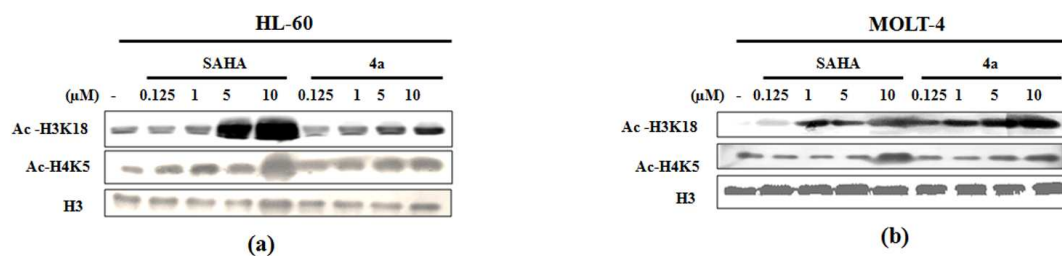


Figure 4: Increase in acetylation of core histones serves as the marker for HDAC Inhibition. (a) **4a** increased the acetylation level of core histones H3 and H4 in HL-60 cells (b) **4a** increased the acetylation level of core histones H3 and H4 in MOLT-4 cells.

4a is least cytotoxic to non-cancerous normal cell lines

Cytotoxicity of **4a** was also evaluated against non-cancerous normal cell line fR-2 and MCF 10a. Interestingly, **4a** was found to be least cytotoxic against fR-2. **4a** showed IC₅₀ value of 23.0

1
2
3 $\pm 2 \mu\text{M}$ against fR-2 and $37 \pm 1 \mu\text{M}$ which is several fold higher than IC_{50} values against
4 different cancer cell lines. Thus **4a** showed selective cytotoxic behavior against cancer cell lines
5 as compared to normal cell line. Importantly, this selective cytotoxicity of **4a** towards cancer cell
6 lines as compared to normal cell lines is an essential pharmacological feature with therapeutic
7 implications. SAHA was used as positive control which showed IC_{50} of 16 ± 1 against fR-2 and
8 $28 \pm 1 \mu\text{M}$ against MCF 10A.
9

18 ***In vivo* anti-leukemic efficacy of 4a**

20 2.5×10^6 P388 lymphocytic cells were injected intraperitoneally in CDF1 female mice weighing
21 18-23 g. A group of 7 animals was treated with **4a** at a dose of 50 mg/kg (i.p.) for 9 consecutive
22 days. Although natural product based HDAC inhibitors like TSA, trapoxin and depudecin
23 generally show toxic effects under *in vivo* conditions but no significant toxic effects were
24 observed in animals treated with **4a**. Moreover, **4a** showed the median survival time of 92.47 %
25 at 50mg/kg i.p. dose. Usually HDAC inhibitors derived from natural resources have limited
26 retention time and are unstable under *in vivo* conditions²¹. The effect of 3-hydroxypyrrolidine on
27 pharmacokinetic and pharmacodynamic properties of **4a** may need further elucidation. 5-
28 Fluorouracil (at 20mg/kg i.p. dose) and SAHA (at 50 mg/kg i.p dose) used as positive controls
29 also showed significant median survival time in P388 lymphocytic model.
30
31
32
33
34
35
36
37
38
39
40
41
42
43

44 **4a induced cell death by inducing mitochondrial membrane potential loss**

46 The proton gradient across the inner mitochondrial membrane is required for oxidative
47 phosphorylation and is measured as mitochondrial membrane potential (ψ_m). ψ_m is reflective of
48 intactness and function of mitochondria and any deviation in ψ_m is used as a marker for inner
49 mitochondrial membrane disruption which leads to apoptosis (Figure 5). Using Rh-123 as a
50 fluorescent probe, **4a** was found to induce loss in ψ_m in HL-60 and MOLT-4 cells. Change in ψ_m
51
52
53
54
55
56
57
58
59
60

was quantified by using flow cytometry. In both the cell lines, percentage of cells undergoing loss in ψ_m increased at higher concentrations. Moreover, loss in ψ_m occurred more prominently in MOLT-4 cells as compared to HL-60 cells. **4a** thus disrupts the architecture of inner mitochondrial membrane and initiates intrinsic apoptotic pathway in both the cell lines used. SAHA was used as positive control.

4a induced ROS independent cell death

Reactive oxygen species (ROS) are important agents that promote cell death in cancer cells. Moreover, many HDAC inhibitors like TSA, SAHA and Sodium butyrate have been reported to cause accumulation of reactive oxygen species in transformed cell lines which facilitates cell death of transformed cells²².

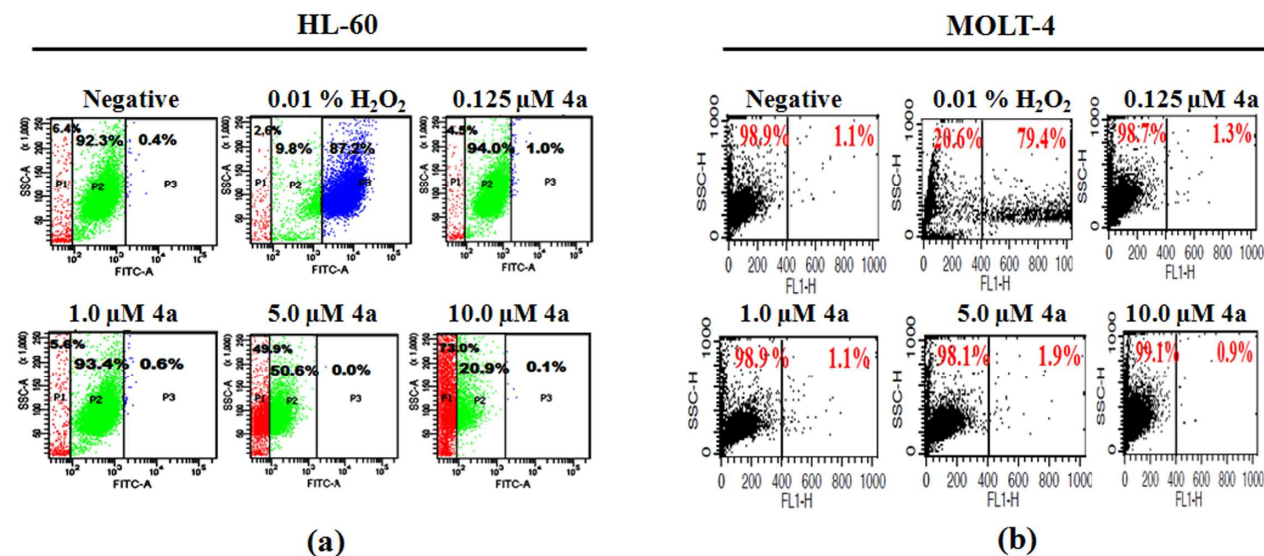


Figure 5: Reactive oxygen species generation was quantified by flow cytometry. H₂O₂ was used as a positive control. H₂DCFDA dye was used as probe. (a) **4a** did not induce accumulation of reactive oxygen species (ROS) in HL-60 cells (b) **4a** did not induce accumulation of reactive oxygen species (ROS) in MOLT-4 cells

We investigated whether **4a** caused generation of ROS by flow cytometry using H₂DCFDA dye as probe. Interestingly, **4a** was not found to induce accumulation of significant level of ROS in

HL-60 and MOLT-4 cells. Thus **4a** induced cell death by ROS independent mechanism (Figure 6). 0.01% H₂O₂ was used as positive control

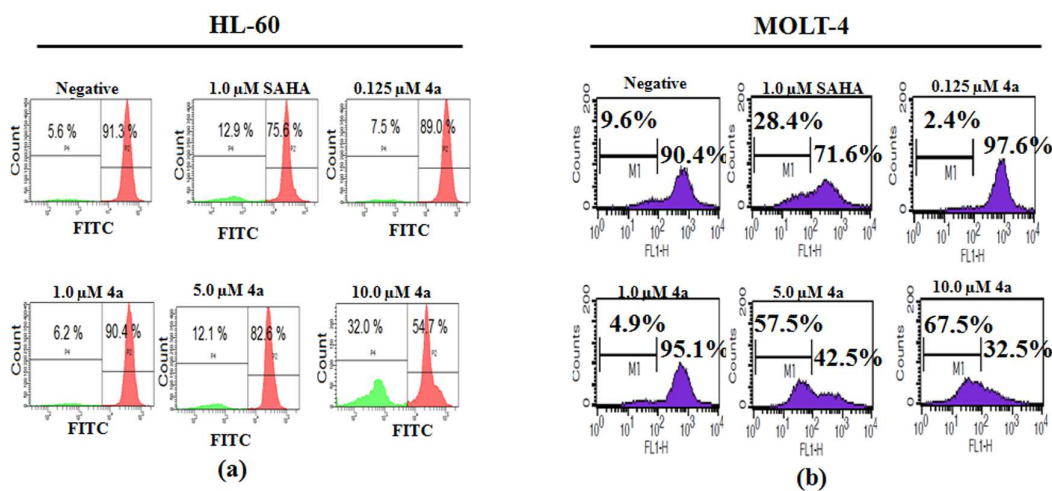


Figure 6: Mitochondrial membrane potential loss was studied by flow cytometry. Rh-123 dye was added half an hour before completion of incubation. (a) **4a** induced mitochondrial membrane potential loss in HL-60 cells (b) **4a** induced mitochondrial membrane potential loss in MOLT-4 cells.

4a induced DNA damage

DNA damage is one of the most important events occurring during cell death. DNA damage serves as the marker of the cell death. Comet assay or Single Cell Gel Electrophoresis (SCGE) assay was used to assess the DNA damage. Comet assay is based on applying electric current to the cells embedded in agarose and lysed by alkaline buffer. The broken DNA fragments migrate away from the nucleus. The resulting fluorescent images, named as comets for their appearance, determine the extent of DNA lesions. Length of tails formed during comet assay depicts the extent of DNA damage induced. DNA damage induction by **4a** was studied in HL-60 cells using comet assay. **4a** was found to induce significant DNA damage in HL-60. Moreover, the extent of damage induced in HL-60 cells by **4a** increased with increase in concentration (Figure 7). DNA damage induced by **4a** was found to be maximum at 10 μ M concentration.

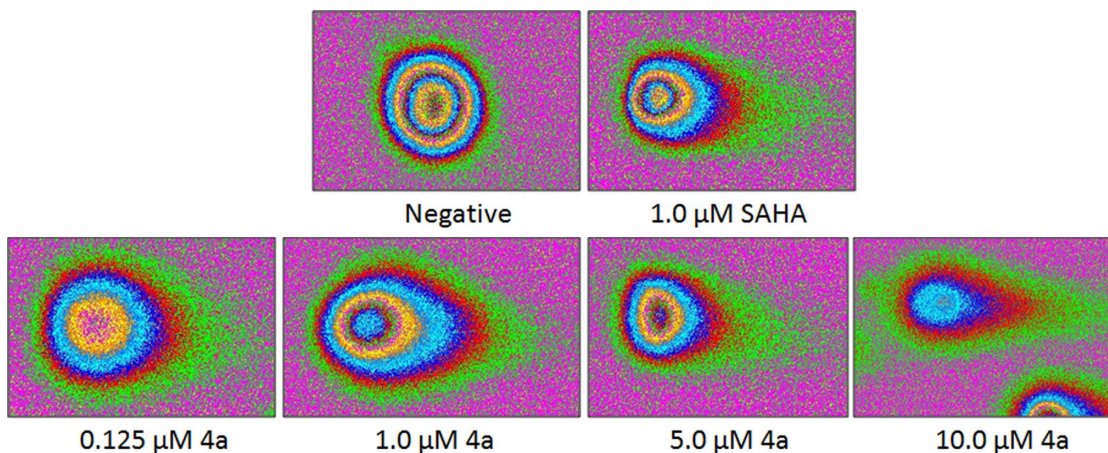


Figure 7: DNA damage induced by **4a** in HL-60 cells was studied by comet assay. Length of tails depicts the damage induced by **4a**.

4a induced autophagy

Autophagy generally promotes tumor suppression. HDAC inhibitors like other cytotoxic agents generally induce autophagy. The characteristic feature of autophagy is the formation of acidic vacuoles. We used acridine orange dye to investigate whether **4a** could induce autophagy. Interestingly, **4a** induced the accumulation of autophagic vacuoles in the cytoplasm of HL-60 and MOLT-4 cells (Figure 8a and 8c). To further confirm induction of autophagy by **4a**, intracellular distribution of LC-3B was detected by immunofluorescent microscopy. In both HL-60 and MOLT-4 cells treated with **4a** punctuated distribution of LC-3B was seen (Figure 8b and 8d). Thus proving that **4a** induced autophagy in HL-60 cells.

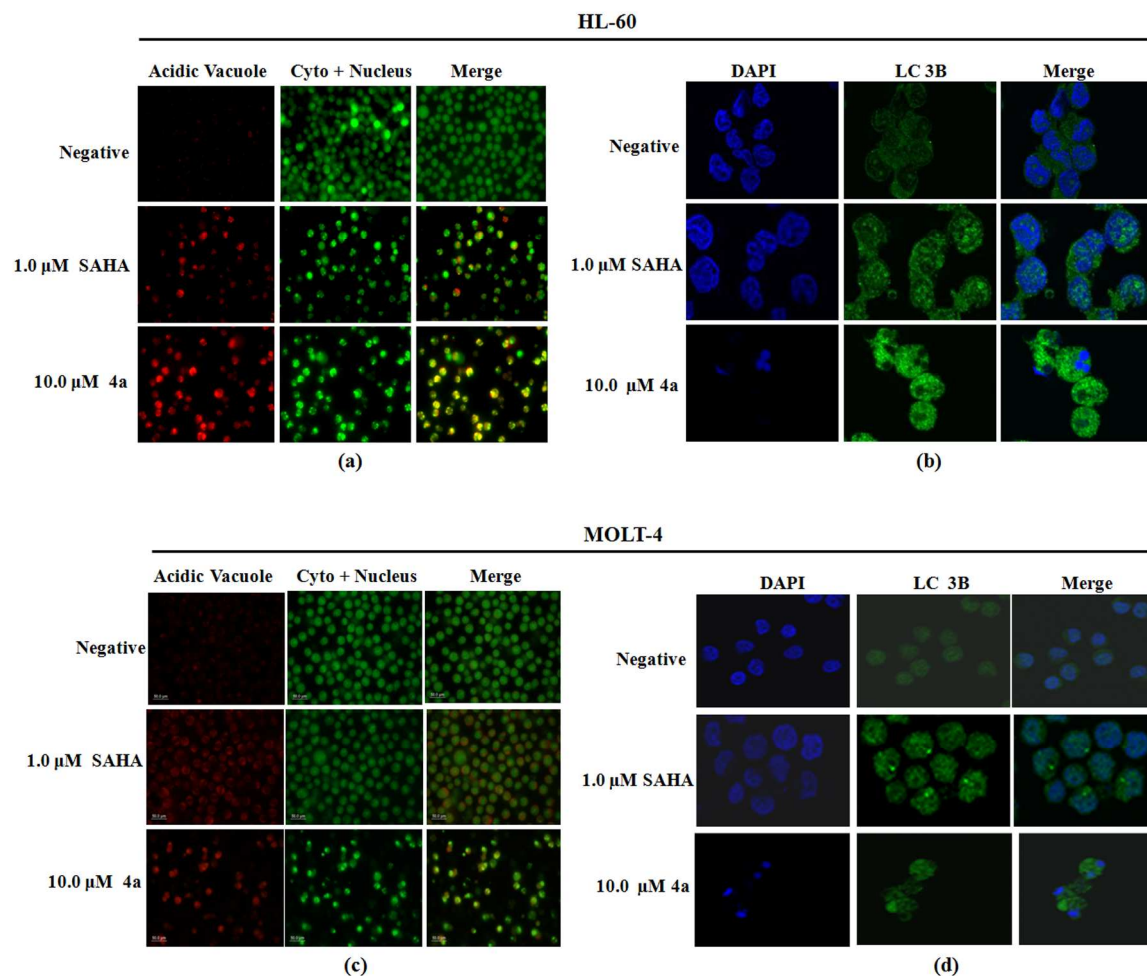


Figure 8. (a) HL-60 cells treated with **4a** were stained with acridine orange dye and examined under fluorescent microscope. **4a** induced formation of acidic vacuoles occurs in cytoplasm. (b) HL-60 cells treated with **4a** were subject to immunofluorescent staining and examined under fluorescent microscope. **4a** caused punctuated distribution of LC-3B. (c) **4a** induced the formation of acidic vacuoles in the cytoplasm of MOLT-4 cells. (d) **4a** induced punctuated distribution of LC-3B in MOLT-4 cells.

4a inhibits cell migration ability of THP-1 cells

Cell motility is a necessary feature for tumor invasion and metastasis^{23,24}. In order to study the effect of **4a** on the migration behavior of cancer cells, cell migration assay was performed (Figure 9). It was found that **4a** prevented the migration of cells to the wounds induced in the confluent monolayers of THP-1 cells. Furthermore, the degree of inhibition of cell migration was found to be higher at higher concentrations. At higher concentrations of **4a**, cell morphology got altered. Migration assay is reflective of potential of an anticancer agent to inhibit metastasis²⁵.

1
2
3
4
5
6
7
8
9
10
11
12
13
14
15
16
17
18
19
20
21
22
23
24
25
26
27
28
29
30
31
32
33
34
35
36
37
38
39
40
41
42
43
44
45
46
47
48
49
50
51
52
53
54
55
56
57
58
59
60

Localization of THP-1 cells induced by **4a** indicated that **4a** may prevent degradation of extracellular matrix proteins and surrounding tissues and may thus inhibit metastasis of cancer cells in *in vivo* models. However, the anti-metastatic ability of **4a** needs further exploration in suitable animal models.

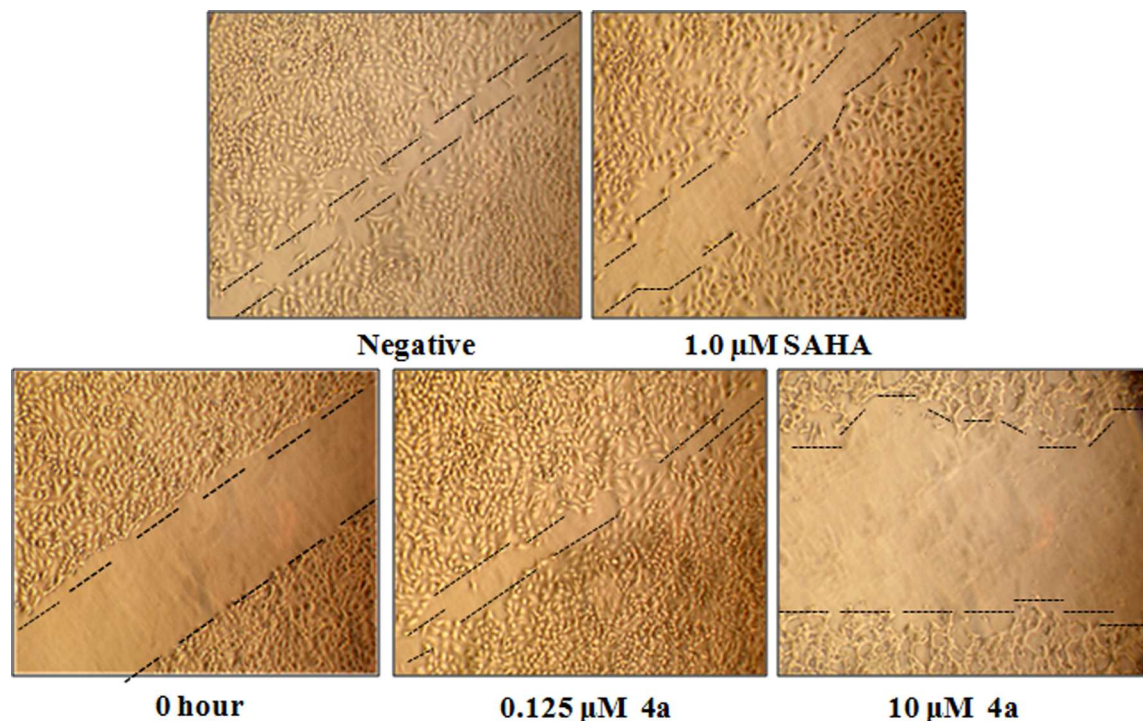


Figure 9: Wound healing assay on THP1 cells. Test molecule addition was carried out after inducing wound in confluent cells. **4a** prevents migration of THP-1 cells.

Conclusion

We in our current study report the designing of a novel HDAC inhibitor (*S*)-*N*¹-hydroxy-*N*⁸-(2-((3-hydroxypyrrolidin-1-yl) methyl) phenyl) octanediamide (**4a**) containing *l*-vasicine derivative 3-hydroxypyrrolidine as a cap group. This is the first time that *l*-vasicine has been used in the synthesis of HDAC inhibitors. Our hypothesis was that *l*-vasicine has essential structural features which may be employed in the designing of novel HDAC inhibitors. During *in silico* studies, molecules containing various derivatives of *l*-vasicine as caps and aliphatic linkers of various

1
2
3 lengths showed significant docking scores. Three schemes of target oriented synthesis were
4 framed to synthesise these probable HDAC inhibitors. Interestingly, 3-hydroxypyrrolidine cap
5 based molecule **4a** with linker length equal to six carbons was found to significantly inhibit
6 enzyme activity of HDACs and induce cell death in different cancer cell lines. **4a** was found to
7 be more specific towards class I HDAC isoforms. HDAC inhibition activity of **4a** was also
8 confirmed by increase in acetylation level of histones in **4a** treated HL-60 and MOLT-4 cells. 3-
9 hydroxypyrrolidine cap was found to be highly sensitive to linker length and any change in
10 linker length rendered molecule inactive. Importantly, **4a** showed several fold higher IC₅₀ value
11 against non-cancerous normal cell line fR-2 and MCF 10A as compared to most cancer cell lines,
12 thus indicating that **4a** induced cancer specific cell death. Moreover, unlike many other natural
13 product based HDAC inhibitors **4a** was found to be non-toxic during *in vivo* studies on P388
14 lymphocytic model. Mechanistic studies revealed that **4a** facilitated cell death by several
15 pathways. **4a** promoted cell death by inducing mitochondrial membrane potential loss and
16 autophagy in HL-60 and MOLT-4 cells. However unlike many HDAC inhibitors **4a** treatment
17 did not lead to accumulation of ROS in HL-60 cells thus inducing ROS independent cell death.
18 Importantly, **4a** showed DNA damage which is an important event in initiating cell death in
19 cancer cells and serves as a key marker for cell death detection. In addition, migration assay
20 showed that **4a** induces localization in THP-1 cells and decreased their ability to migrate to the
21 wound induced in the THP-1 monolayer, thus indicating anti-metastatic potential of **4a**.
22 Moreover, molecular modeling studies revealed that **4a** that cap, linker and chelator of **4a**
23 interact with the different amino acids in the binding pockets of HDACs 2 and 8. However, the
24 hydrophobic cleft formed by Met274, Cys275 and Phe207 provides an additional stability to **4a**
25
26
27
28
29
30
31
32
33
34
35
36
37
38
39
40
41
42
43
44
45
46
47
48
49
50
51
52
53
54
55
56
57
58
59
60

1
2
3 for HDAC8 which is not seen in HDAC-2. From this analysis it was concluded that the molecule
4
5 **4a** has more potency for HDAC-8.
6
7

8 Thus our results indicate designing of a novel HDAC inhibitor (**4a**) employing 3-
9
10 hydroxypyrrolidine derivative of quinazoline alkaloid *l*-vasicine as the cap group. Moreover, the
11
12 cytotoxicity of **4a** against a spectrum of cancer cells of different tissue origins and significantly
13
14 high specificity against cancer cell lines are scientifically valuable results which warrants further
15
16 exploration. **4a** is thus a lead candidate with a therapeutic potential. Moreover, importance of **4a**
17
18 also lies in understanding its unique mechanism of action essentially the fact that unlike other
19
20 HDAC inhibitors it does not produce ROS and is non-toxic to *in vivo* models unlike many
21
22 natural product based HDAC inhibitors. Furthermore, it will be interesting to evaluate the
23
24 applicability of 3-hydroxypyrrolidine cap in HDAC inhibitors containing chelators other than
25
26 hydroxamic acid. Also the effect of 3-hydroxypyrrolidine cap on bioavailability of **4a** may be
27
28 studied.
29
30
31
32
33

34 35 **Experimental Procedure:**

36
37
38 **Chemistry.** ¹H and ¹³C NMR spectra were recorded on Bruker 400 and 500 MHz spectrometers
39
40 with TMS as the internal standard. Chemical shifts are expressed in ppm. ESI-HRMS are
41
42 recorded on a (Agilent Technology 6540 UHD, Acurrat Mass Q-TOF-Lc-Ms) instrument. Silica
43
44 gel coated aluminium plates were used for TLC. Optical rotations were measured on Perkin-
45
46 Elmer 241 polarimeter. Reagents and solvents used were mostly of LR grade. Dry Solvents were
47
48 procured from Merck. HPLC analysis was done on Shimadzu HPLC system (model: LC-6AD)
49
50 equipped with a PDA detector (model: SPD-M20A) using Hypersil BDS C18 (5.0 μ, 4.6 mm ×
51
52 250 mm) column. Mobile phase used was ACN: Buffer (40:60) isocratic elution at flow rate of 1
53
54
55
56
57
58
59
60

1
2
3 ml/min. The purity of final compounds was determined by HPLC. All compounds have $\geq 95\%$
4
5
6
7 purity.

8 **Buffer Preparation:** Dissolve 13.61 g of potassium dihydrogen phosphate in 500 ml of water.
9
10 Shake well to mix and adjust the pH to 2.8 ± 0.05 with dilute orthophosphoric acid. Shake well to
11
12 mix and sonicate to degas.

13
14 **Synthesis of (S)-1-(2-aminobenzyl) pyrrolidin-3-ol (2).** The natural (-)-vasicine (**1**) (10g, 53
15
16 mmol) was dissolved in 100 mL of MeOH/H₂O (1:1) in a 250 mL of round bottom flask with
17
18 continuous stirring, followed by the addition of NaBH₄ (5.87g , 158 mmol) in small amounts
19
20 over a period of 1 h. The mixture was stirred for an additional 1 h, and then extracted with
21
22 CH₂Cl₂ (3x100 mL). The solvent was dried over anhydrous Na₂SO₄ and removed *in vacuo* to
23
24 give the compound (**2**) in 99% yield (10.1 g) as a light yellow semi-solid, $[\alpha]_D^{25} = -199$ (c 3,
25
26 CHCl₃). ¹H NMR (500 MHz, CDCl₃) δ 1.63-1.79 (m, 1H), 2.1-2.2 (m, 1H), 2.24-2.30 (m, 1H),
27
28 2.4-2.6 (m, 2H), 2.73-2.84 (m, 1H), 3.60 (dd, 2H), 4.22-4.38 (m, 1H), 6.6-6.74 (m, 2H), 7.00
29
30 (d, 1H), 7.07 (t, 1H). ¹³C NMR (100 MHz, CDCl₃) δ 34.9, 52.4, 59.1, 62.6, 71.1, 115.6, 117.8,
31
32 123.5, 128.3, 129.8, 146.2. HRMS (+ESI): calc. for C₁₁H₁₆N₂OH 193.1341; found 193.1343.
33
34
35
36
37
38

39 **A: General procedure for boric acid coupling:**

40
41 **(S)-Methyl-8-((2-((3-hydroxypyrrolidin-1-yl)methyl)phenyl)amino)-8-oxooctanoate (3a):**

42
43 Suberic acid monomethyl ester (1 g, 5.32 mmol) and 20 mol% boric acid was weighed into
44
45 reaction vessel, followed by mounting on assembly of a micro-Soxhlet apparatus loaded with
46
47 activated 3Å molecular sieves under nitrogen. Dry toluene (15 mL) and (S)-1-(2-
48
49 aminobenzyl)pyrrolidin-3-ol (**2**) (1 g, 5.23 mmol) then added to reaction vessel and the reaction
50
51 heated to reflux. The mixture was allowed to reflux for 3 h before being concentrated *in vacuo*.
52
53
54
55 The residue was then redissolved in ethyl acetate (20 mL), washed with brine (15 mL), solvent
56
57
58
59
60

dried over anhydrous Na_2SO_4 and removed *in vacuo*. The residue obtained after evaporation was chromatographed over silica gel column using hexane/ethyl acetate (70:30) as eluent to give the compound (**3a**) in 80% yield (1.55 g) as a light yellow semi-solid. ^1H NMR (400 MHz, CDCl_3) δ 8.23 (d, $J = 8.0$ Hz, 1H), 7.27-7.22 (m, 1H), 7.02 (d, $J = 6.5$ Hz, 1H), 6.93 (td, $J = 7.4, 1.0$ Hz, 1H), 4.42 (ddt, $J = 7.5, 5.1, 2.5$ Hz, 1H), 3.74-3.62 (m, 6H), 3.61 (d, $J = 2.9$ Hz, 3H), 2.82 (dt, $J = 11.0, 9.5$ Hz, 1H), 2.63 (ddd, $J = 10.7, 10.4, 3.6$ Hz, 2H), 2.42-2.21 (m, 5H), 2.21-2.14 (m, 1H), 1.82-1.61 (m, 3H), 1.60 (dd, $J = 14.5, 7.4$ Hz, 2H), 1.43-1.27 (m, 4H). ^{13}C NMR (100 MHz, CDCl_3) δ 174.3, 171.6, 138.5, 129.0, 128.2, 126.1, 123.2, 121.0, 70.7, 62.1, 59.1, 52.0, 51.4, 38.1, 34.7, 33.9, 28.8, 28.7, 25.4, 24.6. HRMS (+ESI): calc. for $\text{C}_{20}\text{H}_{30}\text{N}_2\text{O}_4\text{H}$ 363.2284; found 363.2279.

(S)-Methyl-9-((2-((3-hydroxypyrrolidin-1-yl)methyl)phenyl)amino)-9-oxononanoate (3b):

Prepared by the general procedure A and purified on silica gel (ethyl acetate/hexane: 30/70) to obtain the semi-solid product (75%). ^1H NMR (400 MHz, CDCl_3) δ 8.19 (t, $J = 8.5$ Hz, 1H), 7.28-7.12 (m, 1H), 7.05 (d, $J = 6.9$ Hz, 1H), 6.93 (dt, $J = 7.4, 3.7$ Hz, 1H), 4.41 (bs, 1H), 3.63 (t, $J = 5.5$ Hz, 2H), 3.62 (s, 3H), 2.89-2.74 (m, 1H), 2.34 (ddt, $J = 25.1, 15.0, 8.6$ Hz, 6H), 2.20-2.04 (m, 1H), 1.81-1.70 (m, 1H), 1.70-1.61 (m, 2H), 1.58 (dd, $J = 13.2, 7.4$ Hz, 2H), 1.44-1.21 (m, $J = 6$ Hz). ^{13}C NMR (100 MHz, CDCl_3) δ 174.3, 171.7, 154.0, 138.6, 128.9, 128.2, 126.1, 123.1, 120.6, 70.8, 62.2, 59.3, 52.0, 51.4, 51.4, 48.0, 42.6, 36.0, 34.8, 34.0, 25.6, 25.1, 24.8, 23.4, 22.5, 22.5, 20.9. HRMS (+ESI): calc. for $\text{C}_{21}\text{H}_{32}\text{N}_2\text{O}_4\text{H}$ 377.2440; found 377.2438.

(S)-Methyl-5-((2-((3-hydroxypyrrolidin-1-yl)methyl)phenyl)amino)-5-oxopentanoate (3c):

Prepared by the general procedure A and purified on silica gel (ethyl acetate/hexane: 30/70) to obtain the semi-solid product (80%). ^1H NMR (400 MHz, CDCl_3) δ 8.06 (d, $J = 8.2$ Hz, 1H), 7.08 (d, $J = 7.4$ Hz, 1H), 6.89 (d, $J = 7.5$ Hz, 1H), 6.79 (t, $J = 7.3$ Hz, 1H), 4.25 (s, 1H), 3.59 (d, $J =$

1
2
3 12.8 Hz, 1H), 3.48 (s, 3H), 3.41 (d, $J = 12.8$ Hz, 1H), 2.73 (d, $J = 8.7$ Hz, 1H), 2.63 (d, $J = 9.9$ Hz,
4 1H), 2.32 (dd, $J = 10.1, 4.9$ Hz, 1H), 2.23 (dd, $J = 14.2, 7.1$ Hz, 4H), 2.16-2.00 (m, 3H), 1.95-1.80
5 (m, 2H). ^{13}C NMR (100 MHz, CDCl_3) δ 174.1, 170.7, 138.5, 129.0, 128.3, 126.2, 123.3, 120.8,
6 70.9, 62.4, 59.2, 52.0, 51.7, 37.2, 34.7, 33.1, 23.4, 21.1. HRMS (+ESI): calc. for $\text{C}_{17}\text{H}_{24}\text{N}_2\text{O}_4\text{H}$
7 321.1214; found 321.1217.

8
9
10
11
12
13
14 **(S)-Methyl 6-((2-((3-hydroxypyrrolidin-1-yl)methyl)phenyl)amino)-6-oxohexano-ate (3d):**

15
16 Prepared by the general procedure A and purified on silica gel (ethyl acetate/hexane: 30/70) to
17 obtain the semi-solid product (80%). ^1H NMR (400 MHz, CDCl_3) δ 8.21 (d, $J = 8.3$ Hz, 1H), 7.33-
18 7.15 (m, 1H), 7.04 (d, $J = 6.4$ Hz, 1H), 6.94 (dt, $J = 7.2, 6.3$ Hz, 1H), 4.43 (qd, $J = 4.4, 2.0$ Hz,
19 1H), 3.74 (d, $J = 21.2$, 1H), 3.65 (d, $J = 12.5$ Hz, 4H), 2.88 (td, $J = 8.7, 5.2$ Hz, 1H), 2.71 (d, $J =$
20 10.3 Hz, 1H), 2.54 (dd, $J = 10.1, 5.3$ Hz, 1H), 2.45-2.26 (m, 5H), 2.24-2.01 (m, 2H), 1.84-1.58 (m,
21 4H). ^{13}C NMR (100 MHz, CDCl_3) δ 174.2, 171.2, 138.6, 129.0, 128.3, 126.0, 123.2, 120.8, 70.8,
22 62.3, 59.1, 51.9, 51.6, 37.9, 34.7, 33.6, 25.2, 24.4. HRMS (+ESI): calc. for $\text{C}_{12}\text{H}_{26}\text{N}_2\text{O}_4\text{H}$
23 335.1971; found 335.1973.

24
25
26
27
28
29
30
31
32
33
34
35
36 **B: General procedure for hydroxamic acid synthesis.**

37
38 **(S)- N^1 -Hydroxy- N^8 -(2-((3-hydroxypyrrolidin-1-yl)methyl)phenyl)octanediamide (4a):**

39
40 Hydroxylamine hydrochloride (3.51 g, 5.1 mol) in methanol (10 mL) was mixed with KOH (2.83
41 gm, 0.051 mol) at 40 °C in methanol (20 mL) and filtered. The compound (3a) (1g, 2.76 mmol)
42 was then added to the filtrate followed by the addition (over 30 min) of KOH (231 mg, 4.1 mmol).
43
44 The reaction mixture was stirred at room temperature for 6 h. The mixture was added to stirring
45 cold water (90 mL), pH adjusted to 7 by adding acetic acid, followed by the extraction with ethyl
46 acetate. Solvent was dried over anhydrous Na_2SO_4 and removed *in vacuo*. The residue obtained
47
48 after evaporation of the ethyl acetate was chromatographed over silica gel column using
49
50
51
52
53
54
55
56
57
58
59
60

1
2
3 chloroform/methanol (85:15) as eluent to give the compound (**4a**) in 82% yield (820 mg) as a light
4 yellow semi-solid. HPLC: $t_R = 25.6$ min (99% purity). ^1H NMR (400 MHz, $\text{DMSO-}d_6$) δ 10.74
5 (bs, 1H), 8.23 (d, $J = 8.0$ Hz, 1H), 7.30-7.25 (m, 1H), 7.09 (d, $J = 6.5$ Hz, 1H), 6.98 (dt, $J = 7.4$,
6 1.0 Hz, 1H), 4.46 (ddt, $J = 7.5, 5.1, 2.5$ Hz, 1H), 3.78-3.66 (dd, $J = 12.2, 8.1$ Hz, 2H), 2.82 (dt, $J =$
7 12.0, 9.5 Hz, 1H), 2.66 (ddd, $J = 15.7, 10.4, 3.6$ Hz, 2H), 2.46-2.27 (m, 5H), 2.26-2.15 (m, 1H),
8 1.86-1.69 (m, 3H), 1.63 (dd, $J = 14.5, 7.4$ Hz, 2H), 1.46-1.30 (m, 4H). ^{13}C NMR (100 MHz,
9 MeOD) δ 172.3, 171.7, 138.5, 129.1, 128.3, 126.2, 123.3, 121.0, 62.2, 59.1, 52.0, 51.5, 38.1, 34.7,
10 33.9, 28.8, 28.7, 25.5, 24.7. HRMS (+ESI): calc. for $\text{C}_{19}\text{H}_{29}\text{N}_3\text{O}_4\text{H}$ 364.2236; found 364.2233.

11
12
13
14
15
16
17
18
19
20
21
22 **(S)- N^1 -Hydroxy- N^9 -(2-((3-hydroxypyrrolidin-1-yl)methyl)phenyl)nonanediamide (**4b**):**

23 Prepared by the general procedure B and purified on silica gel (chloroform/methanol: 85/15) to
24 obtain the semi-solid product (70%). HPLC: $t_R = 27.2$ min (98% purity). ^1H NMR (400 MHz,
25 DMSO- d_6) δ 10.85 (bs, 1H), 8.21 (t, $J = 8.4$ Hz, 1H), 7.30-7.21 (m, 1H), 7.08 (d, $J = 6.7$ Hz, 1H),
26 6.98 (dt, $J = 7.3, 3.5$ Hz, 1H), 4.45 (s, 1H), 3.68 (t, $J = 5.4$ Hz, 2H), 2.92-2.75 (m, 1H), 2.37 (ddt, J
27 = 25.1, 15.0, 8.5 Hz, 6H), 2.24-2.08 (m, 1H), 1.84-1.74 (m, 1H), 1.74-1.65 (m, 2H), 1.62 (dd, $J =$
28 14.1, 7.0 Hz, 2H), 1.49-1.25 (m, $J = 6\text{H}$). ^{13}C NMR (100 MHz, MeOD) δ 173.2, 171.7, 154.1,
29 138.6, 128.9, 128.2, 126.2, 123.1, 120.7, 62.3, 59.3, 52.1, 51.5, 51.4, 48.1, 42.7, 36.1, 34.8, 34.0,
30 25.7, 25.2, 24.8, 23.5, 22.5, 22.5, 20.9. HRMS (+ESI): calc. for $\text{C}_{20}\text{H}_{32}\text{N}_3\text{O}_4\text{H}$ 378.2393; found
31 378.2389.

32
33
34
35
36
37
38
39
40
41
42
43
44
45 **(S)- N^1 -Hydroxy- N^5 -(2-((3-hydroxypyrrolidin-1-yl)methyl)phenyl)glutaramide (**4c**):** Prepared

46 by the general procedure A and purified on silica gel (methanol/chloroform: 15/85) to obtain the
47 semi-solid product (72%). HPLC: $t_R = 22.4$ min (97% purity). ^1H NMR (400 MHz, $\text{DMSO-}d_6$) δ
48 10.72 (bs, 1H), 8.09 (d, $J = 8.4$ Hz, 1H), 7.12 (d, $J = 7.6$ Hz, 1H), 6.92 (d, $J = 7.6$ Hz, 1H), 6.81 (t,
49 $J = 7.5$ Hz, 1H), 4.28 (s, 1H), 3.61 (d, $J = 13.1$ Hz, 1H), 3.45 (d, $J = 13.2$ Hz, 1H), 2.78 (d, $J = 8.6$
50
51
52
53
54
55
56
57
58
59
60

1
2
3 Hz, 1H), 2.66 (d, $J = 10.1$ Hz, 1H), 2.36 (dd, $J = 10.5, 5.2$ Hz, 1H), 2.27 (dd, $J = 14.4, 7.2$ Hz,
4
5 4H), 2.12-2.02 (m, 3H), 1.97-1.83 (m, 2H). ^{13}C NMR (100 MHz, MeOD) δ 173.0, 170.7, 138.5,
6
7 129.1, 128.3, 126.2, 123.3, 120.9, 70.9, 62.5, 59.2, 52.0, 51.7, 37.2, 34.8, 33.1, 23.4, 21.2. HRMS
8
9 (+ESI): calc. for $\text{C}_{16}\text{H}_{23}\text{N}_3\text{O}_4\text{H}$ 322.1767; found 322.1771.

10
11
12 **(S)-N¹-Hydroxy-N⁶-(2-((3-hydroxypyrrolidin-1-yl)methyl)phenyl)adipamide (4d):** Prepared
13
14 by general procedure A and purified on silica gel (methano/chloroform: 15/85) to obtain the semi-
15
16 solid product (70%). HPLC: $t_R = 23.8$ min (98% purity). ^1H NMR (400 MHz, $\text{DMSO}-d_6$) δ 10.89
17
18 (bs, 1H), 8.25 (d, $J = 8.1$ Hz, 1H), 7.35-7.12 (m, 1H), 7.08 (d, $J = 6.6$ Hz, 1H), 6.98 (td, $J = 7.4,$
19
20 1.0 Hz, 1H), 4.46 (qd, $J = 4.7, 2.1$ Hz, 1H), 3.79 (dd, $J = 12, 11.1$ Hz, 1H), 3.65 (d, $J = 12.5$ Hz,
21
22 4H), 2.90 (dt, $J = 8.7, 5.0$ Hz, 1H), 2.74 (d, $J = 10.4$ Hz, 1H), 2.57 (dd, $J = 10.4, 5.1$ Hz, 1H),
23
24 2.48-2.28 (m, 5H), 2.27-2.05 (m, 2H), 1.88-1.61 (m, 4H). ^{13}C NMR (100 MHz, MeOD) δ 173.2,
25
26 171.3, 138.6, 129.0, 128.3, 126.1, 123.2, 120.8, 70.9, 62.3, 59.1, 51.9, 51.6, 37.9, 34.7, 33.6, 25.3,
27
28 24.48. HRMS (+ESI): calc. for $\text{C}_{17}\text{H}_{25}\text{N}_3\text{O}_4\text{H}$ 336.1923; found 336.1912.

29
30
31
32
33
34 **C: (R)-1-Benzylpyrrolidin-3-amine (7):** (S)-1-Benzylpyrrolidin-3-ol (1 g, 5.68 mmol) and TEA
35
36 (170.4 mg, 1.136 mmol) were added to DCM (50 mL) at 0 °C. A solution of tosyl chloride (1.62
37
38 g, 8.52 mmol) in DCM (30 mL) was added dropwise. The reaction mixture was stirred at 0 °C
39
40 for 30 min then at room temperature for 12 h. Water (50 mL) was added and the organic phase
41
42 washed with saturated solution of NaHCO_3 (2x50 mL), followed by brine. The organic layer was
43
44 collected and dried over anhydrous Na_2SO_4 and the solvent evaporated under reduced pressure to
45
46 obtain tosyl alcohol (6). The compound (6) (4 mmol), sodium azide (520 mg, 8.0 mmol) and
47
48 tetrabutylammonium bromide (5 mol %) in DMF (5 mL) are stirred for 6 h at 60 °C. It was then
49
50 cooled to room temperature and then triphenylphosphine (1.153 g, 4.4 mmol) added to it and
51
52 stirred overnight at room temperature. The resultant mixture was then poured into water (100
53
54
55
56
57
58
59
60

1
2
3 mL) and extracted with DCM (2x10 mL). The acid and base treatments given to the DCM layer
4
5 to partially purify the product. The organic phase was dried over anhydrous Na₂SO₄ and
6
7 removed *in vacuo* to obtain the crude compound, which was chromatographed over silica gel
8
9 column using chloroform/methanol (85:15) as eluent to give the compound (7) in 60% yield (600
10
11 mg) as a light yellow liquid, $[\alpha]_D^{25} = -1.92$ (neat). ¹H NMR (400 MHz, CDCl₃) δ 7.43-7.15 (m,
12
13 5H), 3.64 (q, *J* = 12.8 Hz, 2H), 3.51 (s, 1H), 2.72 (dd, *J* = 7.8, 5.0 Hz, 2H), 2.47 (dd, *J* = 14.3,
14
15 7.4 Hz, 1H), 2.30 (dd, *J* = 15.0, 10.1 Hz, 1H), 2.27-2.12 (m, 1H), 1.48 (d, *J* = 5.0 Hz, 1H). ¹³C
16
17 NMR (100 MHz, CDCl₃) δ 138.4, 128.7, 128.3, 127.2, 58.8, 52.8, 52.2, 51.5, 34.8. HRMS
18
19 (+ESI): calc. for C₁₁H₁₇N₂H 177.1392; found 177.1386.

20
21
22
23
24
25
26 **(R)-Methyl 5-((1-benzylpyrrolidin-3-yl)amino)-5-oxopentanoate (8a):** Prepared by the
27
28 general procedure A and purified on silica gel (ethyl acetate/hexane: 30/70) to obtain a semi-
29
30 solid product (80%). ¹H NMR (400 MHz, CDCl₃) δ 7.28 (m, 5H), 4.44 (s, 1H), 3.68-3.50 (m,
31
32 5H), 2.88 (m, 1H), 2.64-2.48 (m, 2H), 2.25 (t, *J* = 7.2 Hz, 3H), 2.07 (dd, *J* = 16.1, 9.1 Hz, 2H),
33
34 1.74 (s, 4H). ¹³C NMR (100 MHz, CDCl₃) δ 173.6, 172.1, 133.8, 129.9, 128.7, 128.5, 128.3,
35
36 59.0, 58.9, 52.1, 51.5, 51.4, 33.5, 33.1, 20.9, 20.8. HRMS (+ESI): calc. for C₁₇H₂₄N₂O₃H
37
38 305.1265; found 305.1264.

39
40
41
42
43
44 **(R)-Methyl-6-((1-benzylpyrrolidin-3-yl)amino)-6-oxohexanoate (8b):** Prepared by the
45
46 general procedure A and purified on silica gel (ethyl acetate/Hexane: 30/70) to obtain a semi-
47
48 solid product (80%). ¹H NMR (500 MHz, CDCl₃) δ 7.32-7.15 (m, 5H), 6.03 (s, 1H), 4.41 (dd, *J*
49
50 = 6.6, 2.1 Hz, 1H), 3.65-3.64 (m, 4H), 3.60 (d, *J* = 3.8 Hz, 1H), 2.92 (dd, *J* = 13.7, 8.5 Hz, 1H),
51
52 2.59 (dd, *J* = 11.0, 2.8 Hz, 1H), 2.51 (dd, *J* = 11.0, 3.2 Hz, 1H), 2.37-2.24 (m, 4H), 2.14 (t, *J* =
53
54 6.1 Hz, 2H), 1.70-1.57 (m, 5H). ¹³C NMR (101 MHz, CDCl₃) δ 173.9, 172.0, 136.8, 129.1,
55
56
57
58
59
60

1
2
3 128.4, 127.5, 60.0, 59.8, 52.4, 51.4, 48.1, 36.0, 33.6, 32.9, 25.0, 24.3. HRMS (+ESI): calc. for
4
5 $C_{12}H_{26}N_2O_3H$ 319.2022; found 319.2017.
6
7

8
9 **(R)-Methyl-8-((1-benzylpyrrolidin-3-yl) amino)-8-oxooctanoate (8c):** Prepared by the
10 general procedure A and purified on silica gel (ethyl acetate/hexane: 30/70) to obtain a semi-
11 solid product (80%). 1H NMR (400 MHz, $CDCl_3$) δ 7.27-6.93 (m, 5H), 4.38 (s, 1H), 3.55 (dd, J
12 = 22.1, 7.7 Hz, 5H), 2.65 (d, J = 11.2 Hz, 1H), 2.51 (dd, J = 11.4, 7.1 Hz, 1H), 2.37 (t, J = 7.40
13 Hz, 2H), 2.32-2.21 (m, 4H), 2.10- 2.00 (m, 2H), 1.55-1.45 (m, 6H), 1.20 (m, 4H). ^{13}C NMR (100
14 MHz, $CDCl_3$) δ 173.2, 172.6, 136.1, 129.3(2C), 128.4(2C), 127.7, 59.8, 59.5, 52.3, 51.4, 47.9,
15 36.4, 33.9, 31.9, 28.7, 28.7, 25.4, 24.6. HRMS (+ESI): calc. for $C_{20}H_{30}N_2O_3H$ 347.2335; found
16 347.2332.
17
18
19
20
21
22
23
24
25
26
27

28 **(R)-Methyl 9-((1-benzylpyrrolidin-3-yl)amino)-9-oxononanoate (8d):** Prepared by the
29 general procedure A and purified on silica gel (ethyl acetate/hexane: 30/70) to obtain a semi-
30 solid product (80%). 1H NMR (500 MHz, $CDCl_3$) δ 7.41-7.23(m, 5H), 4.49-4.39 (m, 1H), 3.70
31 (d, J = 13.2 Hz, 1H), 3.61 (d, J = 13 Hz, 1H), 3.59 (d, J = 2.4 Hz, 3H), 3.00 (td, J = 8.4, 3.1 Hz,
32 1H), 2.62 (d, J = 10.0 Hz, 1H), 2.42 (dd, J = 10.6, 6.2 Hz, 1H), 2.28-2.19 (m, 1H), 2.17-2.05 (m,
33 4H), 1.98-1.88 (m, 2H), 1.65 (dt, J = 11.1, 7.0, 1H), 1.54-1.45 (m, 4H), 1.21-1.16 (m, 5H). ^{13}C
34 NMR (100 MHz, MeOD) δ 174.3, 172.3, 137.6, 128.9(2C), 128.2(2C), 127.2, 60.3, 59.8, 52.4,
35 51.3, 48.2, 36.5, 34.5, 31.9, 27.9, 28.6, 25.3, 24.6, 24.7. HRMS (+ESI): calc. for $C_{21}H_{33}N_2O_3H$
36 361.2491; found 361.2488.
37
38
39
40
41
42
43
44
45
46
47
48

49 **(R)- N^1 -(1-benzylpyrrolidin-3-yl)- N^5 -hydroxyglutaramide (9a):** Prepared by the general
50 procedure B and purified on silica gel (methanol/chloroform: 15/85) to obtain a semi-solid
51 product (68%). HPLC: t_R = 29.6 min (97% purity). 1H NMR (400 MHz, $DMSO-d_6$) δ 10.89 (bs,
52 1H), 7.30 (dd, J = 4.5, 6.1 Hz, 5H), 4.48 (s, 1H), 3.72-3.54 (m, 5H), 2.92 (m, 1H), 2.68- 2.51 (m,
53
54
55
56
57
58
59
60

1
2
3 2H), 2.29 (t, $J = 7.4$ Hz, 3H), 2.10 (dd, $J = 16.5, 8.8$ Hz, 2H), 1.79 (s, 4H). ^{13}C NMR (100 MHz,
4 MeOD) δ 172.6, 172.1, 133.8, 129.9, 128.7, 128.5, 128.4, 59.1, 58.9, 52.1, 51.5, 51.5, 33.5, 33.2,
5
6
7 20.9, 20.8. HRMS (+ESI): calc. for $\text{C}_{16}\text{H}_{24}\text{N}_3\text{O}_3\text{H}$ 306.1212; found 306.1216.
8
9

10
11 **(R)- N^1 -(1-benzylpyrrolidin-3-yl)- N^6 -hydroxyadipamide (9b):** Prepared by the general
12 procedure A and purified on silica gel (methanol/chloroform: 15/85) to obtain a semi-solid
13 product (75%). HPLC: $t_R = 30.8$ min (99% purity). ^1H NMR (500 MHz, $\text{DMSO}-d_6$) δ 10.99 (bs,
14 1H), 7.41-7.17 (m, 5H), 6.08 (s, 1H), 4.46 (dd, $J = 6.2, 2.3$ Hz, 1H), 3.67 (d, $J = 5.3$ Hz, 1H),
15 3.62 (d, $J = 13.8$ Hz, 1H), 2.92 (dd, $J = 13.9, 8.5$ Hz, 1H), 2.62 (dd, $J = 10.0, 2.3$ Hz, 1H), 2.55
16 (dd, $J = 10.0, 6.4$ Hz, 1H), 2.31 (dt, $J = 14.0, 6.5$ Hz, 4H), 2.14 (t, $J = 6.9$ Hz, 2H), 1.68-1.58 (m,
17 5H). ^{13}C NMR (100 MHz, MeOD) δ 172.9, 172.1, 136.8, 129.2(2C), 128.4(2C), 127.6, 59.7,
18 52.4, 48.1, 36.1, 33.7, 32.1, 25.0, 24.4. HRMS (+ESI): calc. for $\text{C}_{17}\text{H}_{25}\text{N}_3\text{O}_3\text{H}$ 320.1974; found
19 320.1970.
20
21
22
23
24
25
26
27
28
29
30
31

32
33 **(R)- N^1 -(1-benzylpyrrolidin-3-yl)- N^8 -hydroxyoctanediamide (9c):** Prepared by the general
34 procedure B and purified on silica gel (methanol/chloroform: 15/85) to obtain a semi-solid
35 product (70%). HPLC: $t_R = 32.2$ min (99% purity). ^1H NMR (400 MHz, $\text{DMSO}-d_6$) δ 11.11 (bs,
36 1H), 7.43-7.05 (m, 5H), 4.50 (s, 1H), 3.7 (d, $J = 13$ Hz, 1H), 3.62 (d, $J = 13.0$ Hz, 1H), 2.71 (d, J
37 = 10.2 Hz, 1H), 2.58 (dd, $J = 10.2, 6.6$ Hz, 1H), 2.44 (t, $J = 7.4$ Hz, 2H), 2.38-2.28 (m, 4H),
38 2.15-2.04 (m, 2H), 1.65-1.52 (m, 6H), 1.32-1.26 (m, 4H). ^{13}C NMR (100 MHz, MeOD) δ 173.2,
39 172.7, 136.2, 129.4(2C), 128.5(2C), 127.8, 59.6, 52.4, 51.4, 48.0, 36.4, 33.9, 32.0, 28.8, 28.8,
40 25.4, 24.7. HRMS (+ESI): calc. for $\text{C}_{19}\text{H}_{29}\text{N}_3\text{O}_3\text{H}$ 348.2287; found 348.2283.
41
42
43
44
45
46
47
48
49
50
51

52
53 **(R)- N^1 -(1-benzylpyrrolidin-3-yl)- N^9 -hydroxynonanediamide (9d):** Prepared by the general
54 procedure B and purified on silica gel (methanol/chloroform: 15/85) to obtain a semi-solid
55
56
57
58
59
60

1
2
3 product (80%). HPLC: $t_R = 33.3$ min (98% purity). ^1H NMR (500 MHz, $\text{DMSO-}d_6$) δ 10.02 (s,
4 1H), 7.38-7.26 (m, 5H), 4.53 (dd, $J = 7.2, 3.1$ Hz, 1H), 3.76 (d, $J = 12.8$ Hz, 1H), 3.67 (d, $J =$
5 7.5 Hz, 1H), 3.07 (td, $J = 9.0, 3.7$ Hz, 1H), 2.78 (d, $J = 10.3$ Hz, 1H), 2.61 (dd, $J = 10.4, 6.7$ Hz,
6 1H), 2.42-2.34 (m, 1H), 2.33-2.26 (m, 4H), 2.14-2.07 (m, 2H), 1.71 (ddd, $J = 12.9, 8.2, 4.0$ Hz,
7 1H), 1.65-1.57 (m, 4H), 1.31-1.27 (m, 5H). ^{13}C NMR (100 MHz, MeOD) δ 173.2, 172.5, 137.7,
8 129.0(2C), 128.4(2C), 127.4, 59.9, 52.6, 48.3, 36.7, 34.0, 32.4, 29.0, 28.9, 25.6, 24.9, 24.9.
9
10
11
12
13
14
15
16
17
18
19
20
21
22
23
24
25
26
27
28
29
30
31
32
33
34
35
36
37
38
39
40
41
42
43
44
45
46
47
48
49
50
51
52
53
54
55
56
57
58
59
60

HRMS (+ESI): calc. for $\text{C}_{20}\text{H}_{32}\text{N}_3\text{O}_3\text{H}$ 362.2444; found 362.2442.

(S)-1-Benzylpyrrolidin-3-amine (14): Prepared by the general procedure C and purified on silica gel (methanol/chloroform: 15/85) to obtain a yellow liquid (50%), $[\alpha]_D^{25} = +1.90$ (neat). ^1H NMR (400 MHz, CDCl_3) δ 7.41-7.19 (m, 5H), 3.61 (q, $J = 12.8$ Hz, 2H), 3.51 (s, 1H), 2.72 (dt, $J = 14.3, 7.2$ Hz, 2H), 2.47 (dd, $J = 14.9, 8.7$ Hz, 1H), 2.31 (dd, $J = 9.3, 4.3$ Hz, 1H), 2.20 (dt, $J = 13.7, 8.3$ Hz, 1H), 1.49 (d, $J = 5.9$ Hz, 1H). ^{13}C NMR (100 MHz, CDCl_3) δ 138.4, 128.7(2C), 128.3(2C), 127.2, 58.8, 52.7, 52.1, 51.4, 34.7. HRMS (+ESI): calc. for $\text{C}_{11}\text{H}_{17}\text{N}_2\text{H}$ 177.1392; found 177.1389.

(S)-Methyl 5-((1-benzylpyrrolidin-3-yl)amino)-5-oxopentanoate (15a): Prepared by the general procedure A and purified on silica gel (ethyl acetate/Hexane: 30/70) to obtain a semi-solid product (80%). ^1H NMR (500 MHz, CDCl_3) δ 7.43- 7.28 (m, 5H), 4.47 (s, 1H), 3.68-3.58 (m, 5H), 2.79 (s, 1H), 2.68-2.51 (m, 1H), 2.41-2.19 (m, 5H), 2.11 (t, $J = 7.4$ Hz, 1H), 1.92-1.85 (m, 3H), 1.78 (d, $J = 11.3$ Hz, 1H). ^{13}C NMR (125 MHz, CDCl_3) δ 173.6, 172.0, 133.7, 129.8, 128.8, 128.4, 128.3, 59.0, 58.9, 52.0, 51.5, 51.4, 33.4, 33.0, 20.8, 20.7. HRMS (+ESI): calc. for $\text{C}_{17}\text{H}_{24}\text{N}_2\text{O}_3\text{H}$ 305.1265; found 305.1259.

1
2
3 **(S)-Methyl 6-((1-benzylpyrrolidin-3-yl)amino)-6-oxohexanoate (15b):** Prepared by the
4 general procedure A and purified on silica gel (ethyl acetate/hexane: 30/70) to obtain a semi-
5 solid product (80%). ¹H NMR (500 MHz, CDCl₃) δ 7.27-7.19 (m, 5H), 4.45 (m, 1H), 3.69-3.47
6 (m, 5H), 2.99-2.88 (m, 1H), 2.64 (d, *J* = 11.5 Hz, 1H), 2.51 (dd, *J* = 11.8, 6.0 Hz, 1H), 2.31- 2.19
7 (m, 4H), 2.12-2.01 (m, 2H), 1.69-1.54 (m, 5H). ¹³C NMR (100 MHz, CDCl₃) δ 173.9, 172.0,
8 136.7, 129.1, 128.3, 127.5, 60.1, 59.6, 52.4, 51.4, 48.1, 36.0, 33.6, 32.0, 25.0, 24.3. HRMS
9 (+ESI): calc. for C₁₂H₂₆N₂O₃H 319.2022; found 319.2016.
10
11
12
13
14
15
16
17
18
19

20
21 **(S)-Methyl-8-((1-benzylpyrrolidin-3-yl)amino)-8-oxooctanoate (15c):** Prepared by the
22 general procedure A and purified on silica gel (ethyl acetate/hexane: 30/70) to obtain a semi-
23 solid product (80%). ¹H NMR (400 MHz, CDCl₃) δ 7.31 (m, 5H), 4.55 (m, 1H), 3.76-3.60 (m,
24 5H), 3.04 (s, 1H), 2.75 (d, *J* = 10.4 Hz, 1H), 2.66 (dd, *J* = 10.2, 6.6 Hz, 1H), 2.35-2.29 (m, 4H),
25 2.15-2.09 (m, 3H), 1.65 (s, 3H), 1.38 (dd, *J* = 14.9, 11.1 Hz, 5H). ¹³C NMR (100 MHz, CDCl₃) δ
26 173.9, 172.5, 138.2, 128.5, 127.9, 126.8, 60.3, 59.8, 52.5, 51.2, 48.1, 35.9, 33.6, 31.8, 28.5, 28.5,
27 25.3, 24.8. HRMS (+ESI): calc. for C₂₀H₃₀N₂O₃H 347.2335; found 347.2338.
28
29
30
31
32
33
34
35
36
37

38
39 **(S)-Methyl 9-((1-benzylpyrrolidin-3-yl)amino)-9-oxononanoate (15d):** Prepared by the
40 general procedure A and purified on silica gel (ethyl acetate/hexane: 30/70) to obtain a semi-
41 solid product (80%). ¹H NMR (500 MHz, CDCl₃) δ 7.27-7.24 (m, 3H), 7.21 (s, 2H), 4.30-460
42 (m, 1H), 3.73-3.58 (m, 5H), 3.00-2.81 (m, 1H), 2.63-2.53 (m, 1H), 2.49 (dd, *J* = 11.4, 7.3 Hz,
43 1H), 2.29-2.19 (m, 5H), 2.11-1.97 (m, 2H), 1.61-1.47 (m, 5H), 1.31-1.16 (m, 5H). ¹³C NMR (125
44 MHz, CDCl₃) δ 173.8, 172.3, 137.2, 128.5, 127.8, 126.9, 59.9, 59.5, 52.2, 50.9, 47.7, 36.0, 33.5,
45 31.6, 28.5, 28.4, 28.4, 25.0, 24.3. HRMS (+ESI): calc. for C₂₁H₃₃N₂O₃H 361.2491; found
46 361.2489.
47
48
49
50
51
52
53
54
55
56
57
58
59
60

1
2
3
4
5
6
7
8
9
10
11
12
13
14
15
16
17
18
19
20
(S)-N¹-(1-benzylpyrrolidin-3-yl)-N⁵-hydroxyglutaramide (16a): Prepared by the general procedure B and purified on silica gel (methanol/chloroform: 15/85) to obtain a semi-solid product (74%). HPLC: $t_R = 29.5$ min (99% purity). ¹H NMR (500 MHz, DMSO-*d*₆) δ 10.58 (s, 1H), 7.52-7.29 (m, 5H), 4.57 (s, 1H), 3.79-3.62 (m, 2H), 2.89 (s, 1H), 2.73-2.59 (m, 1H), 2.46-2.26 (m, 5H), 2.12 (t, $J = 7.4$ Hz, 1H), 2.01-1.85 (m, 3H), 1.78 (d, $J = 13.1$ Hz, 1H). ¹³C NMR (125 MHz, MeOD) δ 172.1, 172.0, 133.8, 129.9, 128.7, 128.5, 128.4, 58.9, 52.1, 51.5, 51.5, 33.5, 33.2, 21.0, 20.8. HRMS (+ESI): calc. for C₁₆H₂₄N₃O₃H 306.1212; found 306.1215.

21
22
23
24
25
26
27
28
29
30
31
32
33
34
35
36
37
38
39
40
(S)-N¹-(1-benzylpyrrolidin-3-yl)-N⁶-hydroxyadipamide (16b): Prepared by the general procedure B and purified on silica gel (methanol/chloroform: 15/85) to obtain a semi-solid product (76%). HPLC: $t_R = 30.9$ min (97% purity). ¹H NMR (500 MHz, DMSO-*d*₆) δ 10.99 (s, 1H), 7.33-7.26 (m, 5H), 6.48 (d, $J = 7.0$ Hz, 1H), 4.50 (td, $J = 10.8, 8.4$ Hz, 1H), 3.71 (d, $J = 12.8$ Hz, 1H), 3.64 (d, $J = 12.9$ Hz, 1H), 3.06-2.95 (m, 1H), 2.71 (d, $J = 10.3$ Hz, 1H), 2.59 (dd, $J = 10.3, 6.6$ Hz, 1H), 2.38-2.23 (m, 4H), 2.17-2.09 (m, 2H), 1.75-1.63 (m, 5H). ¹³C NMR (101 MHz, MeOD) δ 172.8, 172.0, 136.9, 129.2, 128.4, 127.6, 59.7, 52.4, 51.5, 48.1, 36.1, 33.7, 32.1, 25.0, 24.4. HRMS (+ESI): calc. for C₁₇H₂₅N₃O₃H 320.1974; found 320.1972.

41
42
43
44
45
46
47
48
49
50
51
52
53
54
55
56
57
58
59
60
(S)-N¹-(1-benzylpyrrolidin-3-yl)-N⁸-hydroxyoctanediamide (16c): Prepared by the general procedure B and purified on silica gel (methanol/chloroform: 15/85) to obtain a semi-solid product (72%). HPLC: $t_R = 32.0$ min (99% purity). ¹H NMR (400 MHz, DMSO-*d*₆) δ 11.07 (s, 1H), 7.29 (d, $J = 16.4$ Hz, 5H), 4.51 (s, 1H), 3.71 (t, $J = 8.5$ Hz, 1H), 3.65 (d, $J = 13.0$ Hz, 1H), 3.00 (s, 1H), 2.71 (d, $J = 10.4$ Hz, 1H), 2.59 (dd, $J = 10.2, 6.6$ Hz, 1H), 2.33-2.23 (m, 4H), 2.22-2.09 (m, 3H), 1.62 (s, 3H), 1.35-1.12 (m, 5H). ¹³C NMR (101 MHz, CDCl₃) δ 173.0, 172.5,

1
2
3 138.2, 128.6, 128.0, 126.9, 59.9, 52.6, 51.2, 48.1, 36.1, 33.7, 31.8, 28.6, 28.6, 25.3, 24.9. HRMS
4
5 (+ESI): calc. for C₁₉H₂₉N₃O₃H 348.2287; found 348.2284.
6
7

8
9 **(S)-N⁷-(1-benzylpyrrolidin-3-yl)-N⁹-hydroxynonanediamide (16d)**: Prepared by the general
10 procedure B and purified on silica gel (methanol/chloroform: 15/85) to obtain a semi-solid
11 product (80%). HPLC: *t_R* = 33.5 min (97% purity). ¹H NMR (500 MHz, DMSO-*d*₆) δ 10.65 (s,
12 1H), 7.35-7.30 (m, 3H), 7.26 (s, 2H), 4.48 (m, 1H), 3.66-3.59 (m, 2H), 3.02- 2.87 (m, 1H), 2.70-
13 2.60 (m, 1H), 2.56 (dd, *J* = 10.1, 6.5 Hz, 1H), 2.36-2.24 (m, 5H), 2.12-2.06 (m, 2H), 1.69-1.53
14 (m, 5H), 1.35-1.24 (m, 5H). ¹³C NMR (125 MHz, CDCl₃) δ 172.9, 172.3, 137.2, 128.6, 127.9,
15 126.9, 59.5, 50.9, 47.8, 36.1, 35.8, 33.6, 31.7, 28.6, 28.5, 28.5, 25.2, 24.4. HRMS (+ESI): calc.
16 for C₂₀H₃₂N₃O₃H 362.2444; found 362.2438.
17
18
19
20
21
22
23
24
25
26
27

28 ***In silico* screening and molecular modeling studies on HDACs.**

29
30 All the molecular modelling studies of 3-hydroxy pyrrolidine and amino-1-benzyl pyrrolidine
31 molecules on HDAC were performed by using Schrodinger suite 2015. The X-ray crystal
32 structure information of HDAC isoforms 1, 4 and 8 were gathered and the structures were
33 downloaded from Protein Data Bank (PDB). All the structure were properly analysed and PDB
34 Id 4BKX (HDAC-1:apo protein), 2VQM (HDAC-4:bound with N-hydroxy-5-[(3-phenyl-5,6-
35 dihydroimidazo[1,2-a]pyrazin-7(8H)-yl)carbonyl]thiophene-2-carboxamide) 5IWG (HDAC-2:
36 bound with BRD4884) and 1VKG (HDAC-8: bound with CRAA-A) were retrieved for
37 molecular docking studies. To conduct molecular docking studies the protein was optimized and
38 minimized using OLS-2005 force-field to attain stable conformation of the protein with
39 minimum energy and less constrains. In case of HDAC-1, the co-ordinate information of bound
40 ligand from HDAC-8 was considered to define binding pocket where as in case 2, 4 and 8 the co-
41 ordinates of co-crystallized ligands were taken to define the active site of the protein and grid
42
43
44
45
46
47
48
49
50
51
52
53
54
55
56
57
58
59
60

1
2
3 was generated. Before performing docking studies the docking protocol was standardized where
4 this co-crystallized ligand was prepared and re-docked at XP (Extra precision) and SP (Standard
5 precision) using glide module of Schrodinger. On comparing the conformation of the co-
6 crystallized ligands with its docked poses to their respective proteins, it was observed that XP
7 mode docking reproduces the bio-active conformation of the bound ligand (with RMSD less than
8 2Å°). Thus further molecular docking studies were performed at XP^{26, 27, 28, 29}.

17 **Cell lines, growth medium and treatment conditions.**

19 The cell lines THP-1, HL-60, Colo-205 and Caco-2, MIAPaCa-2, PC-3, A549 MCF-7 and fR-2
20 were procured from European Collection of Cell Cultures (ECACC), UK. THP-1, HL-60, Colo-
21 205, Caco-2, A549 and fR-2 cell lines were maintained in RPMI-1640 medium supplemented
22 with 10% FCS. A549, MIAPaCa-2 and MCF-7 were maintained in DMEM medium
23 supplemented with 10% FCS. All Culture media wwere supplemented with 1% pencillin. Cells
24 were cultured at 37⁰C in CO₂ incubator (New Brunswick, Galaxy 170R, eppendroff) with
25 internal atmosphere conditions of 95% humidity and 5% CO₂ gas.
26
27
28
29
30
31
32
33
34
35

36 **Cell lines, growth medium and treatment conditions.**

38 The cell lines THP-1, HL-60, Colo-205 and Caco-2, MIAPaCa-2, PC-3, A549 MCF-7 and fR-2
39 were procured from European Collection of Cell Cultures (ECACC), UK. THP-1, HL-60, Colo-
40 205, Caco-2, A549 and fR-2 cell lines were maintained in RPMI-1640 medium supplemented
41 with 10% FCS. A549, MIAPaCa-2 and MCF-7 were maintained in DMEM medium
42 supplemented with 10% FCS. All Culture media were supplemented with 1% pencillin. Cells
43 were cultured at 37⁰C in CO₂ incubator (New Brunswick, Galaxy 170R, eppendroff) with internal
44 atmosphere conditions of 95% humidity and 5% CO₂ gas. H3K18 and H4K5 antibodies were
45
46
47
48
49
50
51
52
53
54
55
56
57
58
59
60

1
2
3 procured from Cell Signaling Technology, USA and H3 antibody was procured from Biovision
4 CA,USA.
5
6

7 **Cytotoxicity assay.**

8
9
10 The effect of test molecules on cell proliferation potential was evaluated by MTT assay.
11 Adherent cells were seeded in 96 well plates 12 hours before test molecule addition while as
12 suspension cell lines were seeded in 96 well plates 4 hours prior to drug addition. After 48 hours
13 exposure to different concentrations of test molecules, 20 μ l of MTT was added to each well and
14 incubated for further 4 hours. In case of adherent cells, media was removed by tapping 96 well
15 plates slowly on blotting sheets and then 150 μ l DMSO was added to each well. In case of
16 suspension cell lines, first 96 well plates were centrifuged at 3000 rpm for 15 minutes and then
17 media was removed like in case of adherent cells. After this 150 μ l DMSO was added to each
18 well. The 96 well plates were placed on the orbital shaker for 10 minutes at medium speed to
19 allow the dissolution of formazon crystals. The absorbance was recorded at the wavelength of
20 570 nm in the micro-plate reader and cytotoxicity was calculated.
21
22
23
24
25
26
27
28
29
30
31
32
33
34
35

36 **Measurement of HDAC activity against HeLa cell nuclear extract.** HDAC inhibition was
37 measured by HDAC fluorometric drug screening kit procured from Biovision (catalogue number
38 K340-100). The kit was used according to manufacturers guide lines. 10mM stocks of test
39 molecules were prepared. The specific concentrations of test molecules were achieved in 85 μ l of
40 double distilled water. 2X reaction mixture was prepared and added to each well of clear bottom
41 black 96 well plates. After this, incubation was done at 37 $^{\circ}$ C for 30 minutes. The reaction was
42 stopped with 10 μ l developer and again incubation was done at 37 $^{\circ}$ C for 30 minutes. Florescence
43 was measured at $\lambda_{\text{excitation}} = 450$ nm and $\lambda_{\text{emission}} = 350$ nm.
44
45
46
47
48
49
50
51
52
53
54
55
56
57
58
59
60

Measurement of HDAC isoform specificity.

HDAC isoform specificity of **4a** was measured by fluorometric HDAC isoform inhibition assay kits procured from BPS biosciences (BPS Bioscience Inc., USA). The kits were used as per manufacturer's instructions. 10 mM stocks of test compounds were prepared. The HDAC reaction mixture was composed of HDAC buffer, BSA, HDACs, appropriate concentration of test compounds and fluorogenic substrate. The reaction mixture was incubated at 37°C for 60 minutes and then reaction was stopped by addition of developer. After 20 minutes of incubation, fluorescence was detected at the excitation wavelength of 360 nm and emission wavelength of 460 nm.

Histone extraction.

Histones were extracted by acid extraction methodology. 10^7 cells were seeded in 100 mm dishes. After 2-4 hours, cells were treated with indicated concentrations of **4a** and SAHA. Incubation was carried for 48 hours. Cells were pelleted and suspended in Histone extraction buffer (10 mM HEPES pH 9, 1.5 mM $MgCl_2$, 10 mM KCl, 0.5 mM DTT and protease inhibitors. DTT was added just prior to use). HCl was added to make final concentration of HCl in the lysate equal to 0.2N. Lysis was carried out on ice for 1 hr. After this, centrifugation was carried out at 11,000g for 10 minutes. Supernatant fraction which contains histones was kept and pellet was discarded. For loading equal amounts of histones on the gel protein estimation by Bradford assay was done.

Western blot assays.

For western blot assays, cells were seeded 2 to 4 hours before treatment with indicated concentrations of **4a** and SAHA. The cells were incubated under normal culture conditions for 48 hours and afterwards cells were centrifuged at 1000 rpm for 10 min. Cells were then rinsed

1
2
3 with ice cold PBS. The histones were extracted by acid extraction methodology Afterwards
4
5 histone samples were denatured by adding β -mercaptoethanol containing loading dye and by
6
7 heating for 5 min at 98°C. They were then resolved on 18% polyacrylamide gels. After blotting
8
9 onto poly-vinylidene difluoride (PVDF) membranes were incubated with antibodies.
10
11 Normalization of cell extracts was performed by staining with rabbit anti- β actin diluted at 1:500.
12
13 Goat anti-rabbit and goat anti-mouse HRP conjugated secondary antibodies were used. Signal
14
15 was detected using immobilon Western Chemiluminescent HRP Substrate and captured by using
16
17 X-ray film.
18
19
20
21

22 **Detection of *in vivo* antitumor efficacy in P388 leukaemia cancer model.**

23
24 P388 lymphocytic leukemia cells grown in the peritoneal cavity of DBA/2 female mice were
25
26 collected from the animal harboring 6-7 days old ascites. For testing, CDF1 females were used.
27
28 5 x 10⁵ cells were injected intraperitoneally in 24 CDF1 females weighing 18-23 g on day 0. The
29
30 next day, animals were randomized and divided into four groups, containing 7 animals each.
31
32 Groups I & II were treated with SAHA and **4a** at the dose of 50mg/kg (i.p.) for 9 consecutive
33
34 days. Group III was treated with 5-fluorouracil (20 mg/kg) (i.p.) and it served as positive
35
36 control. The control group received 0.2 ml normal saline (i.p.) for 9 consecutive days. The
37
38 animals in each group were observed for mortality up to day 18 and the median survival time of
39
40 animals in each group was calculated using the prescribed formula and %T/C values were
41
42 arrived at.
43
44
45
46
47

48 **Measurement of change in mitochondrial membrane potential.**

49
50 HL-60 and MOLT-4 cells were seeded in 6 well plates and were incubated under standard
51
52 culture conditions for 2-4 hours. After this, indicated concentrations of **4a** were added and the
53
54 treated cells were incubated under standard conditions for 48 hours. 1 μ M Rh-123 stain was
55
56
57
58
59
60

1
2
3 added to cells for half an hour before completion of incubation. After cells were centrifuged at
4
5 1000 rpm for 10 minutes and then washed twice PBS. The cells were again suspended in PBS
6
7
8 and the change in membrane potential was quantified by flow cytometry using BD-FACS Aria II
9
10 flow cytometer ((Becton Dickinson, Franklin Lakes, NJ, USA)).

11 12 **Measurement of intracellular reactive oxygen species (ROS) generation.**

13
14
15 HL-60 and MOLT-4 cells were cultured and seeded in six well plates. Different concentrations
16
17 of **4a** were added and incubation was done for 48 h. After 48h, cells were harvested, washed in
18
19 PBS, cells were then incubated in 5 μ M H₂DCFDA reagent for 30 minutes at 37°C. The
20
21 generation of ROS was measured by the change in fluorescence due to the production of 2', 7'-
22
23 dichlorofluorescein (DCF) in FITC channel on BD FACS Aria II Flow Cytometer (Becton
24
25 Dickinson, Franklin Lakes, NJ, USA). 0.01% H₂O₂ used as positive control was added 10
26
27 minutes before PBS washing.
28
29
30

31 32 **Detection of DNA damage by comet assay.**

33
34 Slides were pre-coated with normal melting agarose. A coat of 75 μ l of 0.5% low melting point
35
36 agarose mixed with HL-60 cells was added to these slides. The coverslips were placed on the
37
38 slides and were then kept on a slide tray resting on icepacks until the agarose layers hardened (5-
39
40 10 min). The coverslips were removed and the slides were slowly lowered into cold, freshly
41
42 prepared lysing solution (2.5 M NaCl, 100 mM Na₂EDTA, 10 mM Trizma base, 12 g/l NaOH, 1
43
44 g sodium dodecyl sulphate; pH=10). 1% triton X-100 was added afreshly to solubilize cellular
45
46 proteins. Slides were incubated in the cold lysis buffer for 2h. Electrophoresis was performed
47
48 under pH>13 alkaline conditions at 300 milli amperes and 24 volts (~0.74 V/cm) for 40 min.
49
50 Slides were coated with neutralization buffer (0.4 M Tris, 10 M HCl; pH=7.5) drop wise and
51
52 kept as such for 5 min. Slides were drained the and the neutralization process was repeated twice.
53
54
55
56
57
58
59
60

1
2
3 It was followed by incubating the slides with 80 μ L of 1X ethidium bromide for 5 min. Slides
4
5 were dipped in chilled distilled water to remove excess stain. The coverslips were then placed
6
7 over slides and the slides were examined under an Olympus fluorescence microscope (*IX51*)
8
9 equipped with an excitation filter (510 nm) and a barrier filter (590 nm). The slides were
10
11 analyzed at 40 X magnification using computerized image analysis system (Komet 5.5).
12
13 Approximately 100 cells were scored immediately and assessed for the DNA damage. The assay
14
15 was performed under dim light to prevent any DNA damage which may arise from fluorescent
16
17 white light.
18
19
20
21

22 **Detection of autophagy by acridine orange assay employing fluorescence microscopy.**

23
24 Induction of autophagy was analyzed by staining cells with acridine orange dye. HL-60 cells were
25
26 seeded in six-well plates and treated with different concentrations of **4a** for 48h. 1.0 μ M SAHA
27
28 was used as positive control. The cells were incubated with 1 μ g/ml acridine orange for 15 min
29
30 prior to the termination of the experiment and incubated at 37°C. Then the cells were harvested
31
32 and washed with PBS before analysis on fluorescent microscope (Olympus Fluoview FV1000).
33
34
35

36 **Detection of autophagy by immunofluorescence microscopy.**

37
38 Cultured HL-60 and MOLT-4 cells were seeded in six-well plates, and incubated in the presence
39
40 of different concentrations of **4a** for 48 h. 1.0 μ M SAHA was used as positive control. After
41
42 completion of incubation, cells were washed twice in PBS, attached on poly-lysine coated cover
43
44 slips and fixed in 4% paraformaldehyde for 15 min at room temperature. Cells were
45
46 permeabilized in PBS with 0.1% TritonX-100 at room temperature for 10 min. Nonspecific
47
48 binding sites were blocked by incubating the cells in 10% BSA. Cells were then incubated with
49
50 LC-3B (Sigma) diluted 1:100 in 0.1% Triton X-100 in PBS for 1hr at room temperature and
51
52 Alexa Fluor 488 conjugated secondary antibody (Invitrogen) diluted 1:500 in PBS for 1 h at
53
54
55
56
57
58
59
60

1
2
3 room temperature. Cells were then washed three times in PBS and stained with 4',6-diamidino-2-
4 phenylindole (DAPI) 1µg/ml in PBS. The cover slips were mounted over glass slides and cells
5
6 were imaged by fluorescent microscope (Olympus Fluoview FV1000) by using 60X oil
7
8 immersion objective lens.
9
10

11 12 **Cell migration assay.**

13
14 Cell migration assay is used to study the directional cell migration of cancer cells under invitro
15
16 conditions. THP-1 cells were seeded at high density in 6-well plates and were allowed to attach
17
18 over night under standard culture conditions. A wound was induced in the cell monolayer by
19
20 scratching with sterile 1000 µL tip and images were taken at various intervals including at zero
21
22 time interval. The debris was removed by PBS washes and the desired concentrations of test
23
24 molecule were added. The plates were incubated under standard culture conditions for 48 hours.
25
26 The wounds were photographed at 0 hour and 48 hour and the cell migration was quantified by
27
28 comparing distance between edges of wound.
29
30
31
32
33

34 **ASSOCIATED CONTENT**

35
36 Experimental details including synthesis and characterization data.
37
38

39 **AUTHOR INFORMATION**

40
41 Corresponding authors
42

43
44 *Abid Hamid; Ph.D.
45

46 Cancer Pharmacology Division, CSIR-Indian Institute of Integrative Medicine, Canal Road,
47
48 Jammu-180001, India; CSIR-Academy of Scientific & Innovative Research, New Delhi, Govt.
49
50 of India.
51

52
53 Phone: +91-191-2585006 extn. 381
54

55
56 Cell: +91-9419245425
57
58
59
60

1
2
3 Fax: +91-191-2585333
4

5 E-mail: ahdar@iiim.ac.in
6

7
8 *Subhash Chandra Taneja; Ph.D.
9

10 Natural Product Microbes Division, CSIR-Indian Institute of Integrative Medicine, Canal Road,
11
12 Jammu-180001, India.
13

14
15 Phone: +91-191-2585006 extn. 311
16

17 Fax: +91-191-2585333
18

19
20 Email: sctaneja@iiim.ac.in
21

22 *Bhahwal Ali Shah, Ph. D
23

24 Natural Product Microbes Division, CSIR-Indian Institute of Integrative Medicine, Canal Road,
25
26 Jammu-180001, India, CSIR-Academy of Scientific & Innovative Research, New Delhi, Govt. of
27
28 India.
29

30
31 Phone: +91-191-2585006 extn. 311
32

33
34 Fax: +91-191-2585333
35

36
37 Email: bashah@iiim.ac.in
38

39 **Author contributions**

40
41 ¹These authors contributed equally.
42

43 **Notes**

44
45
46 The authors declare no competing financial interest.
47

48 **Acknowledgments**

49
50 The authors would like to thank Director CSIR-IIIM Jammu, Dr. Ram A Vishwakarma for
51
52 providing the facilities to carry out this work (IIIM/2006/2017). The authors would like to
53
54 acknowledge DBT, New Delhi, India for extramural funding under
55
56
57
58
59
60

1
2
3 BT/PR13140/PBD/17/656/2009 to Abid Hamid. The authors (M.A, M.A.A, J.A.B, A.R. and
4
5 B.K.) thank CSIR/UGC, New Delhi for the award of Senior Research Fellowships.
6
7

8 ABBREVIATIONS

9
10 HDAC, Histone deacetylase; CTCL, chronic T-cell lymphoma; SAHA, suberoylanalide
11
12 hydroxamic acid; SAR, structure activity relationship; IC₅₀, concentration at which cell growth
13
14 or enzyme activity is inhibited by 50%.
15
16

17 ANCILLARY INFORMATION:

18 **Supporting Information Availability:**

- 19
20
21
22
 - 23 • HDAC Inhibition curves of Known Inhibitors
 - 24 • Structure of ligand CRAA-A bound to HDAC-8
 - 25 • NMR Spectra, HRMS Spectra and HPLC Chromatogram Scans
 - 26 • Molecular Formula Strings

27
28
29
30
31
32
33
34
35
36
37
38
39
40
41
42
43
44
45
46
47
48
49
50
51
52
53
54
55
56
57
58
59
60

References

1. Ellis, L.; Atadja, P. W.; Johnstone, R. W. Epigenetics in cancer: targeting chromatin modifications. *Mol. Cancer Ther.* **2009**, *8*, 1409–1420.
2. Heerboth, S.; Housman, G.; Leary, M.; Longacre, M.; Byler, S.; Lapinska, K.; Willbanks, A.; Sarkar, S. EMT and tumor metastasis. *Clinical and Translational Medicine.* **2015**, *4*, 6.
3. Arrowsmith, C. H.; Bountra, C.; Fish, P. V.; Lee, K.; Schapira, M. Epigenetic protein families: a new frontier for drug discovery. *Nat. Rev. Drug Discov.* **2012**, *11*, 384–400.
4. Mohammad, H. P.; Smitheman, K. N.; Kamat, C. D.; Soong, D.; Federowicz, K. E.; Van Aller, G. S.; Schneck, J. L.; Carson, J. D.; Liu, Y.; Butticello, M.; Bonnette, W. G.; Gorman, S. A.; Degenhardt, Y.; Bai, Y.; McCabe, M. T.; Pappalardi, M. B.; Kaspavec, J.; Tian, X.; McNulty, K. C.; Rouse, M.; McDevitt, P.; Ho, T.; Crouthamel, M.; Hart, T. K.; Concha, N. O.; McHugh, C. F.; Miller, W. H.; Dhanak, D.; Tummino, P. J.; Carpenter, C. L.; Johnson, N. W.; Hann, C. L.; Kruger, R. G. A DNA hypomethylation signature predicts antitumor activity of LSD1 inhibitors in sclc. *Cancer Cell.* **2015**, *28*, 57–69.
5. Verdin, E.; Ott, M. 50 Years of protein acetylation: from gene regulation to epigenetics, metabolism and beyond. *Nat. Rev. Mol. Cell Biol.* **2014**, *16*, 258–264.
6. Haberland, M.; Montgomery, R. L.; Olson, E. N. The many roles of histone deacetylases in development and physiology: implications for disease and therapy. *Nat. Rev. Genet.* **2009**, *10*, 32–42.
7. Marks, P. A.; Rifkind, R. A.; Richon, V. M.; Breslow, R.; Miller, T.; Kelly, W. K. Histone deacetylases and cancer: causes and therapies. *Nat. Rev. Cancer.* **2001**, *1*, 194–202.

- 1
2
3
4
5
6
7
8
9
10
11
12
13
14
15
16
17
18
19
20
21
22
23
24
25
26
27
28
29
30
31
32
33
34
35
36
37
38
39
40
41
42
43
44
45
46
47
48
49
50
51
52
53
54
55
56
57
58
59
60
8. Dokmanovic, M.; Clarke, C.; Marks, P. A. Histone deacetylase inhibitors: overview and perspectives. *Mol. Cancer Res.* **2007**, *5*, 981–989.
 9. Rasheed, W. K.; Johnstone, R. W.; Prince, H. M. Histone deacetylase inhibitors in cancer therapy. *Expert Opin. Investig. Drugs.* **2007**, *16*, 659–678.
 10. Fiegler, N.; Textor, S.; Arnold, A.; Rölle, A.; Oehme, I.; Breuhahn, K.; Witzens-harig, M.; Cerwenka, A.; De, W.; Alexander, R.; Moldenhauer, G. Downregulation of the activating NKp30 ligand B7-H6 by HDAC inhibitors impairs tumor cell recognition by NK cells. *Blood.* **2013**, *122*, 684–693.
 11. Minucci, S.; Pelicci, P. G. Histone deacetylase inhibitors and the promise of epigenetic (and more) treatments for cancer. *Nat. Rev. Cancer.* **2006**, *6*, 38–51.
 12. Choudhary, C.; Kumar, C.; Gnad, F.; Nielsen, M. L.; Rehman, M.; Walther, T. C.; Olsen, J. V.; Mann, M. Lysine acetylation targets protein complexes and co-regulates major cellular functions. *Science.* **2013**, *325*, 834–840.
 13. Bradner, J. E.; West, N.; Grachan, M. L.; Greenberg, E. F.; Haggarty, S. J.; Warnow, T.; Mazitschek, R. Chemical phylogenetics of histone deacetylases. *Nat. Chem. Biol.* **2010**, *6*, 238–243.
 14. Ruiz, R.; Raez, L. E.; Rolfo, C. Entinostat (SNDX-275) for the treatment of non-small cell lung cancer. *Expert Opin. Investig. Drugs.* **2015**, *24*, 1101–1109.
 15. Marks, P. A.; Dokmanovic, M. Histone deacetylase inhibitors: discovery and development as anticancer agents. *Expert Opin. Investig. Drugs.* **2005**, *14*, 1497–1511.
 16. Bolden, J. E.; Peart, M. J.; Johnstone, R. W. Anticancer activities of histone deacetylase inhibitors. *Nat. Rev. Drug Discov.* **2006**, *5*, 769–784.

- 1
2
3
4
5
6
7
8
9
10
11
12
13
14
15
16
17
18
19
20
21
22
23
24
25
26
27
28
29
30
31
32
33
34
35
36
37
38
39
40
41
42
43
44
45
46
47
48
49
50
51
52
53
54
55
56
57
58
59
60
17. Xu, W. S.; Parmigiani, R. B.; Marks, P. A. Histone deacetylase inhibitors: molecular mechanisms of action. *Oncogene*. **2007**, *26*, 5541–5552.
18. Wang, D.; Gao, F. Quinazoline derivatives: synthesis and bioactivities. *Chem. Cent. J.* **2013**, *7*, 95.
19. a) Aga, M. A.; Kumar, B.; Rouf, A.; Shah, B. A.; Andotra, S. S.; and Taneja, S. C. Natural (–)-vasicine as a novel source of optically pure 1-benzylpyrrolidin-3-ol. HCA, *Bioorg. Med. Chem.* **2013**, *96*, 969–977. b) Aga, M. A.; Rayees, S.; Rouf, A.; Kumar, B.; Sharma, A.; Nagaraju, P.V.V.S.; Singh, G.; Taneja, S. C. Synthesis of ofornine mimics from natural product l-vasicine as anti-hypertensive agents. *Bioorg. Med. Chem.* **2017**, *25*, 1440-1447.
20. Jia, H.; Morris, C. D.; Williams, R. M.; Loring, J. F.; Thomas, E. A. HDAC inhibition imparts beneficial transgenerational effects in huntington’s disease mice via altered DNA and histone methylation. *Proc. Natl. Acad. Sci.* **2015**, *112*, E56–E64.
21. Ma, W. W.; Adjei, A. A. Novel agents on the horizon for cancer therapy. *CA. Cancer J. Clin.* **2009**, *59*, 111–137.
22. Marks, P. A.; Xu, W. S. Histone deacetylase inhibitors: potential in cancer therapy. *J. Cell Biochem.* **2009**, *107*, 600–608.
23. Wells, A.; Grahovac, J.; Wheeler, S.; Ma, B.; Lauffenburger, D. Targeting tumor cell motility as a strategy against invasion and metastasis. *Trends Pharmacol. Sci.* **2013**, *34*, 283–289.
24. Zhou, H.; H, S. Role of mTOR signaling in tumor cell motility, invasion and metastasis. *Curr. Protein Pept Sci.* **2011**, *12*, 30–42.
25. Kramer, N.; Walzl, A.; Unger, C.; Rosner, M.; Krupitza, G.; Hengstschläger, M.; Dolznig, H. *In vitro* cell migration and invasion assays. *Mutat. Res.* **2013**, *752*, 10–24.

- 1
2
3
4
5
6
7
8
9
10
11
12
13
14
15
16
17
18
19
20
21
22
23
24
25
26
27
28
29
30
31
32
33
34
35
36
37
38
39
40
41
42
43
44
45
46
47
48
49
50
51
52
53
54
55
56
57
58
59
60
26. Di Micco, S.; Chini, M.G.; Terracciano, S.; Bruno, I.; Riccio, R.; Bifulco, G. Structural basis for the design and synthesis of selective HDAC inhibitors. *Bioorg. Med. Chem.* **2013**, *21*, 3795-3807.
27. Sharma, S.; Ahmad, M.; Bhat, J. A.; Kumar, A.; Kumar, M.; Zargar, M.A.; Hamid, A.; Shah, B. A. Design, synthesis and biological evaluation of β -boswellic acid based HDAC inhibitors as inducers of cancer cell death. *Bioorg. Med. Chem.* **2014**, *24*, 4729-4734.
28. Somoza, J. R.; Skene, R. J.; Katz, B. A.; Mol, C.; Ho, J. D.; Jennings, A. J.; Luong, C.; Arvai, A.; Buggy, J. J.; Chi, E.; Tang, J.; Sang, B. C.; Verner, E.; Wynands, R.; Leahy, E.; M.; Dougan, D. R.; Snell, G.; Navre, M.; Knuth, M. W.; Swanson, R. V.; McRee, D. E.; Tari, L. W. Structural snapshots of human HDAC8 provide insights into the class I histone deacetylases. *Structure.* **2004**, *12*, 1325-1334.
29. Millard, C. J.; Watson, P. J.; Celardo, I.; Gordiyenko, Y.; Cowley, S. M.; Robinson, C. V.; Fairall, L.; Schwabe, J. W. Class I HDACs share a common mechanism of regulation by inositol phosphates. *Molecular Cell.* **2013**, *51*, 57-67.

Table of contents graphic

